

# The motion of a fluid ellipsoid in a general linear background flow

By WILLIAM J. MCKIVER AND DAVID G. DRITSCHEL

Mathematical Institute, University of St Andrews, North Haugh, St Andrews KY16 9SS, UK

(Received 11 October 2001 and in revised form 18 July 2002)

The study of the motion of a fluid ellipsoid has a long and fascinating history stretching back originally to Laplace in the late 18th century. Recently, this subject has been revived in the context of geophysical fluid dynamics, where it has been shown that an ellipsoid of uniform potential vorticity remains an ellipsoid in a background flow consisting of horizontal strain, vertical shear, and uniform rotation. The object of the present work is to present a simple, appealing, and practical way of investigating the motion of an ellipsoid not just in geophysical fluid dynamics but in general. The main result is that the motion of an ellipsoid may be reduced to the evolution of a symmetric,  $3 \times 3$  matrix, under the action of an arbitrary  $3 \times 3$  ‘flow’ matrix. The latter involves both the background flow, which must be linear in the Cartesian coordinates at the surface of the ellipsoid, and the self-induced flow, which was given by Laplace.

The resulting simple dynamical system lends itself ideally to both numerical and analytical study. We illustrate a few examples and then present a theory for the evolution of a vortex within a slowly varying background flow. We show that a vortex may evolve quasi-adiabatically, that is, it stays close to an equilibrium form associated with the instantaneous background flow. The departure from equilibrium, on the other hand, is proportional to the rate of change of the background flow.

---

## 1. Introduction

At the turn of the 19th century, there was a great interest in the behaviour of fluid ellipsoids, bodies of fluid having some distinct property bounded by either a free or fixed surface. This work was inspired in part by numerous potential applications but also in part by the mathematical appeal of this simple geometric form. Many great mathematicians were involved, including Dirichlet, Maclaren, Todhunter, Lamb and Chandrasekhar among others (see the book by Chandrasekhar 1969 for a review).

Much more recently, there has been a resurgence of activity in the area of geophysical vortices (Meacham *et al.* 1994; Meacham, Morrison & Flierl 1997; Miyazaki, Ueno & Shimonishi 1999; Hashimoto, Shimonishi & Miyazaki 1999; Miyazaki, Furuichi & Takahashi 2001). This new activity appears to have its genesis in the two-dimensional elliptical vortex model of Moore & Saffman (1971) and Kida (1981). The two-dimensional work was developed in the aeronautical context, for very high Reynolds number incompressible flows, as a simple model of aircraft wake vortices. This model consists essentially of a pair of nonlinear equations governing the evolution of the vortex aspect ratio and orientation. It accounts in general for time-varying background uniform strain and rotation. This model then spread into the geophysical arena, where it has seen widespread use and where, arguably, it is much more

justified due to the robustness of the two-dimensional approximation for large-scale geophysical flows.

The three-dimensional extension of this model was first given by Meacham *et al.* (1994). It was developed under the *quasi-geostrophic* approximation to the full equations governing the motion of a stably stratified, rotating fluid. This approximation is discussed more fully below, but briefly it is considered to be remarkably good under many circumstances. Under this approximation, the flow field is purely horizontal and non-divergent yet in general varies with height. The flow field can thus be recovered from a scalar potential, the streamfunction, and for a uniform vertical profile of the buoyancy frequency, the Laplacian of this streamfunction (after a suitable scaling of the vertical coordinate) equals the *potential vorticity* – a materially invariant scalar field responsible for the entire fluid motion. This is the key connection with the two-dimensional model, where again the potential vorticity (PV) is given by the Laplacian of a streamfunction. It means that the elliptical solutions for uniform PV found by Moore, Saffman and Kida generalize naturally to ellipsoidal solutions in three dimensions (and so on for higher dimensions, should they be relevant).

In the present paper, we begin in §2 by rederiving the equations describing the motion of an ellipsoid under general circumstances. The novelty here is the use of a symmetric  $3 \times 3$  matrix as the prognostic variable. This appears to be the simplest way of writing the equations. We then focus on the quasi-geostrophic model but consistently present the equations, as well as an associated numerical algorithm, in such a way that they can be used for other models of interest. In §3, we examine the background flow arising from a distant vortex or distribution of PV, and then illustrate several examples of vortex evolution in this background flow. We next develop a theory for the motion of an ellipsoid within a weak, slowly varying background flow. This theory is shown to accurately describe the motion of an ellipsoid for long times. A few conclusions and ideas for future work bring the paper to a close in §4.

## 2. Vortex evolution

### 2.1. Motion of an ellipsoid in a background flow

We consider for the moment a linear background flow of the form

$$\mathbf{u}_b(\mathbf{x}, t) = \mathcal{S}_b(t)\mathbf{x}, \quad (1)$$

where  $\mathcal{S}_b$  is a  $3 \times 3$  matrix. Within this flow, we place a single ellipsoidal vortex at the origin and require only that its velocity field has the same form as (1), i.e.  $\mathbf{u}_v = \mathcal{S}_v\mathbf{x}$ . The total velocity field felt by the ellipsoid is

$$\mathbf{u} = \mathcal{S}\mathbf{x} \quad (2)$$

where  $\mathcal{S} = \mathcal{S}_b + \mathcal{S}_v$ , and this depends only on time  $t$ . We refer to  $\mathcal{S}$  as the *flow matrix* subsequently.

The ellipsoid is specified by its axis half-lengths  $a \leq b \leq c$  and the unit vectors  $\hat{\mathbf{a}}$ ,  $\hat{\mathbf{b}}$  and  $\hat{\mathbf{c}}$  directed along these axes (see figure 1). This geometric information may be encapsulated in a single symmetric matrix  $\mathcal{A}$  defined by

$$\mathcal{A} = \mathcal{M}\mathcal{D}\mathcal{M}^T, \quad (3)$$

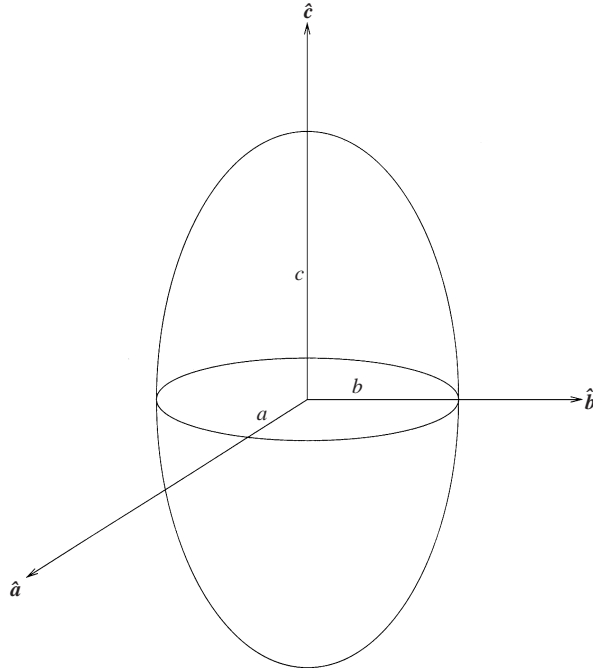


FIGURE 1. Definition of the ellipsoid parameters.

where the superscript  $T$  denotes transpose and the matrices  $\mathcal{M}$  and  $\mathcal{D}$  are given by

$$\mathcal{M} = (\hat{a} \quad \hat{b} \quad \hat{c}), \tag{4a}$$

$$\mathcal{D} = \begin{pmatrix} 1/a^2 & 0 & 0 \\ 0 & 1/b^2 & 0 \\ 0 & 0 & 1/c^2 \end{pmatrix}, \tag{4b}$$

$$\mathcal{M}^T = \begin{pmatrix} \hat{a}^T \\ \hat{b}^T \\ \hat{c}^T \end{pmatrix}. \tag{4c}$$

Here  $\mathcal{M}$  is a rotation matrix and therefore is orthonormal; in particular  $\mathcal{M}^{-1} = \mathcal{M}^T$ .

The equation describing the surface of the ellipsoid is conveniently written as

$$\mathbf{x}^T \mathcal{A} \mathbf{x} = 1. \tag{5}$$

By taking a time derivative of this equation and using  $d\mathbf{x}/dt = \mathbf{u}(\mathbf{x}, t) = \mathcal{P}(t)\mathbf{x}$ , as well as the implied relation  $d\mathbf{x}^T/dt = \mathbf{x}^T \mathcal{P}^T(t)$ , we obtain

$$\mathbf{x}^T \left( \mathcal{P}^T \mathcal{A} + \mathcal{A} \mathcal{P} + \frac{d\mathcal{A}}{dt} \right) \mathbf{x} = 0. \tag{6}$$

Since this must be true for all points  $\mathbf{x}$  on the boundary of the ellipsoid, it follows that

$$\frac{d\mathcal{A}}{dt} = -(\mathcal{P}^T \mathcal{A} + \mathcal{A} \mathcal{P}), \tag{7}$$

which is simply the equation for the evolution of  $\mathcal{A}$  in an arbitrary linear background flow.

Note that  $\mathcal{A}$  remains a symmetric matrix for all time since  $\mathcal{S}^T \mathcal{A} + \mathcal{A} \mathcal{S}$  is automatically symmetric if  $\mathcal{A}$  is.

## 2.2. The quasi-geostrophic ellipsoid

To go further, it is necessary to specify the flow matrix  $\mathcal{S}_v$  in terms of  $\mathcal{A}$ . Here, following previous works (Meacham *et al.* 1994, 1997; Miyazaki *et al.* 1999; Hashimoto *et al.* 1999; Miyazaki *et al.* 2001), we consider the ‘quasi-geostrophic’ (QG) model, which is frequently used to study atmospheric and oceanic flows. The QG equations describe the motion of a rapidly rotating, stably stratified fluid, in the asymptotic limit for which vortices spin slowly relative to the background rotation and for which fluid velocities are small compared to gravity wave speeds (see Gill 1982 for a full description of this system). For an inviscid, adiabatic fluid, the QG equations may be expressed in terms of the conservation of a single material scalar, the ‘potential vorticity’  $q(x, t)$ , i.e.

$$\frac{Dq}{Dt} = \frac{\partial q}{\partial t} + u \frac{\partial q}{\partial x} + v \frac{\partial q}{\partial y} = 0. \quad (8)$$

In the QG model, the vertical velocity  $w = 0$  to this order of approximation, so  $q$  is advected in a layerwise manner. However, the horizontal velocity  $(u, v)$  depends on all three spatial coordinates, and this is recovered from  $q$  via the inversion of

$$\nabla^2 \psi = \frac{\partial^2 \psi}{\partial x^2} + \frac{\partial^2 \psi}{\partial y^2} + \frac{\partial^2 \psi}{\partial z^2} = q \quad (9)$$

for the streamfunction  $\psi$ , followed by the incompressibility relations

$$u = -\frac{\partial \psi}{\partial y}, \quad v = \frac{\partial \psi}{\partial x} \quad (10)$$

in the special case (considered here) when the rotational and buoyancy frequencies  $f$  and  $N$  are constant. This allows one to absorb  $f$  and  $N$  into the height coordinate  $z$  and leaves the operator in (9) isotropic.

In the problem considered here of a single ellipsoidal vortex, we imagine  $q$  being composed of two parts: (i) that due to the vortex itself  $q_v$ , and (ii) that due to external vortices or PV distributions  $q_b$ . Correspondingly,  $\psi = \psi_v + \psi_b$ . The background flow  $\psi_b$  arising from  $q_b$  is not explicitly modelled, but rather we expand  $\psi_b$  in a Taylor series in  $x$ ,  $y$  and  $z$  about the origin (here the centre of the ellipsoid) and truncate this series at second order. The constant part of  $\psi_b$  does not induce any flow and can be ignored while the linear part of  $\psi_b$  induces a uniform flow. Here we adopt a frame of reference moving with this flow so that the ellipsoid remains at the origin. The quadratic part of  $\psi_b$  corresponds to a linear background velocity field, having a flow matrix of the form

$$\mathcal{S}_b = \begin{pmatrix} \partial u_b / \partial x & \partial u_b / \partial y & \partial u_b / \partial z \\ \partial v_b / \partial x & \partial v_b / \partial y & \partial v_b / \partial z \\ 0 & 0 & 0 \end{pmatrix}, \quad (11)$$

where the derivatives are evaluated at the origin. There are only five independent elements of this matrix on account of incompressibility ( $\partial u_b / \partial x + \partial v_b / \partial y = 0$ ), and each element depends on time. For example, if  $\psi_b$  is associated with a single distant vortex (see §3 below), the rotation of the ellipsoid about this vortex, or rather the

mutual rotation of the vortices  $\Omega$ , implies a periodic time dependence. In this case, it is convenient to adopt a frame of reference rotating about the vertical to remove this time dependence; this amounts to adding  $\Omega$  and  $-\Omega$  to  $\partial u_b/\partial y$  and  $\partial v_b/\partial x$  above. Details are given below in §3 for a simple example.

The full flow matrix is the sum of  $\mathcal{S}_b$  and  $\mathcal{S}_v$ , where  $\mathcal{S}_v$  accounts for the self-induced strain. The simple operator relationship between  $\psi$  and  $q$  in (9) means that  $\psi_v$  is a quadratic function of  $x$ ,  $y$  and  $z$  inside the ellipsoid. This immediately implies that  $\mathcal{S}_v$  is spatially uniform, and we need this property to ensure that the ellipsoid remains an ellipsoid. The dependence of  $\mathcal{S}_v$  on the ellipsoidal shape and orientation, for QG flow, was given by Meacham *et al.* (1994), but many details were worked out much earlier and there is a long and interesting history stretching back (at least) to Laplace in 1784 (see Chandrasekhar 1969 and Todhunter 1873). The exact form of  $\psi_v$  inside an ellipsoid of uniform source strength (here the PV) was determined originally by Laplace, and takes the form

$$\psi_v = \frac{1}{2} \mathbf{x}^T \mathcal{M} \mathcal{F} \mathcal{M}^T \mathbf{x}, \quad (12)$$

where

$$\mathcal{F} = \begin{pmatrix} \xi_a & 0 & 0 \\ 0 & \xi_b & 0 \\ 0 & 0 & \xi_c \end{pmatrix} \quad (13)$$

is a diagonal matrix and the coefficients are determined from  $a$ ,  $b$  and  $c$  in terms of elliptic integrals of the second kind:

$$\xi_a = \kappa_v R_D(b^2, c^2, a^2), \quad (14a)$$

$$\xi_b = \kappa_v R_D(c^2, a^2, b^2), \quad (14b)$$

$$\xi_c = \kappa_v R_D(a^2, b^2, c^2), \quad (14c)$$

where  $\kappa_v = \Gamma_v/4\pi$  is the vortex ‘strength’,  $\Gamma_v = \frac{4}{3}\pi abcQ$  is the vortex circulation,  $q_v = Q$  is the uniform PV within the ellipsoid, and

$$R_D(\alpha, \beta, \gamma) \equiv \frac{3}{2} \int_0^\infty \frac{dt}{\sqrt{(t+\alpha)(t+\beta)(t+\gamma)^3}}. \quad (15)$$

Using (12) for  $\psi_v$ , together with  $u_v = -\partial\psi_v/\partial y$  and  $v_v = \partial\psi_v/\partial x$ , it follows that

$$\mathcal{S}_v = \mathcal{L} \mathcal{M} \mathcal{F} \mathcal{M}^T, \quad (16)$$

where

$$\mathcal{L} = \begin{pmatrix} 0 & -1 & 0 \\ 1 & 0 & 0 \\ 0 & 0 & 0 \end{pmatrix}. \quad (17)$$

### 2.3. The complete model

The complete model now consists of the evolution equation (7) for the matrix  $\mathcal{A}$  together with the expressions (11) and (16) for the flow matrices  $\mathcal{S}_b$  and  $\mathcal{S}_v$ . It remains to show how  $\mathcal{S}_v$  can be computed from  $\mathcal{A}$ . Essentially, we need to invert (3) for  $\mathcal{D}$  and  $\mathcal{M}$ . This can be accomplished by solving an eigenproblem, as discussed shortly below, but first it proves convenient to rewrite (7) to evolve not  $\mathcal{A}$  but its inverse  $\mathcal{B} = \mathcal{A}^{-1}$ . Using the fact that the product  $\mathcal{A}\mathcal{B}$  is the identity matrix, it

follows that

$$\begin{aligned}\frac{d\mathcal{B}}{dt} &= -\mathcal{B} \frac{d\mathcal{A}}{dt} \mathcal{B} \\ &= \mathcal{B}(\mathcal{S}^T \mathcal{A} + \mathcal{A} \mathcal{S}) \mathcal{B} \\ &= \mathcal{B} \mathcal{S}^T + \mathcal{S} \mathcal{B},\end{aligned}\tag{18}$$

and moreover

$$\mathcal{B} = \mathcal{M} \mathcal{D}^{-1} \mathcal{M}^T,\tag{19}$$

where  $\mathcal{D}^{-1}$  is simply

$$\mathcal{D}^{-1} = \begin{pmatrix} a^2 & 0 & 0 \\ 0 & b^2 & 0 \\ 0 & 0 & c^2 \end{pmatrix}.\tag{20}$$

Note in particular that  $d\mathcal{B}_{3,3}/dt = 0$  in QG flow—this follows because there is no vertical velocity. The element  $\mathcal{B}_{3,3}$  is the half-height of the vortex squared. Note also that the determinant  $|\mathcal{B}| = |\mathcal{D}^{-1}| = (abc)^2$  is proportional to the squared vortex volume and is also invariant (because QG flow is incompressible).

In order to determine the evolution of the ellipsoid it is necessary to be able to calculate the half-lengths,  $a$ ,  $b$  and  $c$ , and the orientation vectors  $\hat{a}$ ,  $\hat{b}$ , and  $\hat{c}$  of the ellipsoid from the matrix  $\mathcal{B}$ . But equation (19), right multiplied by  $\mathcal{M}$ , together with (20) implies

$$\mathcal{B} \hat{a} = a^2 \hat{a},\tag{21a}$$

$$\mathcal{B} \hat{b} = b^2 \hat{b},\tag{21b}$$

$$\mathcal{B} \hat{c} = c^2 \hat{c}.\tag{21c}$$

Hence the half-lengths and the orientation vectors of the ellipsoid can be found directly from the  $\mathcal{B}$  matrix by solving a simple eigenvalue problem.

#### 2.4. Sketch of the numerical algorithm

The algorithm for determining the evolution of the ellipsoid in a linear background flow can be summarized as follows:

##### (i) Initialization

1. Read in values which determine the initial size and orientation of the ellipsoid, i.e.  $a$ ,  $b$ ,  $c$ ,  $\hat{a}$ ,  $\hat{b}$  and  $\hat{c}$ .
2. Read in the values which determine the background flow  $\mathcal{S}_b$ . For the QG model, there are only five independent terms in (11) because of incompressibility.
3. Calculate the initial components of the  $\mathcal{B}$  matrix from (19).
4. Calculate the elliptic integrals  $\xi_a$ ,  $\xi_b$  and  $\xi_c$  from  $a$ ,  $b$ ,  $c$  using (14) and (15), and hence calculate  $\mathcal{S}_v$  from (16).
5. Add  $\mathcal{S}_v$  to  $\mathcal{S}_b$  to obtain the initial flow matrix  $\mathcal{S}$ .

##### (ii) Integration

1. Integrate the evolution equation (18) for  $\mathcal{B}$  by one time step.
2. Calculate the values for  $a$ ,  $b$ ,  $c$ ,  $\hat{a}$ ,  $\hat{b}$  and  $\hat{c}$  by solving the eigenvalue problem (21).
3. Calculate  $\xi_a$ ,  $\xi_b$  and  $\xi_c$ , and from these  $\mathcal{S}_v$  and  $\mathcal{S} = \mathcal{S}_v + \mathcal{S}_b$ .

##### (iii) Full evolution

Repeat (ii) for desired number of time steps.

Numerically, the elliptic functions  $R_D$  are calculated using the NAG routine S21BCF, and the eigenproblem is solved using the NAG routine F02FAF for a symmetric positive-definite matrix. The time integration is carried out using a fourth-order Runge–Kutta scheme, with a time step  $\Delta t = 0.025/|Q|$ , where  $Q$  is the uniform PV within the ellipsoid (we have taken  $Q = 1$  in the algorithm developed). The integration is highly accurate with this time step, and the procedure is simple enough to run efficiently with smaller time steps if particularly great accuracy is required.

The algorithm has been written in a way that allows for arbitrary flow matrices, not just those that arise in QG flow. As such, it is easy to modify for any other application in which a deforming ellipsoid features. A copy of the algorithm is available at <http://www-vortex.mcs.st-andrews.ac.uk>.

### 3. Examples

In this section, we work through a few simple examples to clarify the nature of the background flow matrix  $\mathcal{S}_b$  and to illustrate some of the rich dynamics that this simple system is capable of uncovering.

The previous studies of Meacham, Miyazaki and coworkers have already indicated that the dynamics of an ellipsoid in a steady background flow can be surprisingly complex. For example, vertical shear alone can lead to chaotic motion (Meacham *et al.* 1997). Here, we look more closely into the origin of the background flow matrix  $\mathcal{S}_b$  to better understand the context of this model.

#### 3.1. The flow generated by a distant vortex

We begin by considering the effect of a single distant vortex, of strength  $\kappa_b (= \Gamma_b/4\pi)$ , centred at  $\mathbf{x} = \mathbf{X}_b$ , on an ellipsoidal vortex located at the origin. For the moment, however, suppose the ellipsoid were centred at  $\mathbf{x} = \mathbf{X}_v$ . Let  $R \equiv |\mathbf{X}_b - \mathbf{X}_v|$ . Then, to leading order in  $1/R$ , the vortices rotate about each other at a rate

$$\Omega = \frac{\kappa_b + \kappa_v}{R^3}; \quad (22)$$

the vortices appear as points to this order of approximation. The shape and internal structure of the vortices do not come into play until  $O(R^{-5})$ , assuming each vortex is reasonably compact. We next adopt a frame of reference rotating about the  $z$ -axis passing through the joint centre of the two vortices, so that  $\mathbf{X}_b$  and  $\mathbf{X}_v$  are fixed. Next, we take  $\mathbf{X}_v = 0$ , i.e. we move the target vortex of interest to the origin. Then, in the vicinity of the origin, the background streamfunction takes the form

$$\psi_b = -\frac{\kappa_b}{R} + \frac{1}{2}\mathbf{x}^T \mathcal{P}_b \mathbf{x} + O(\kappa_b |\mathbf{x}|^3/R^4), \quad (23)$$

where notably the linear terms are absent and the matrix  $\mathcal{P}_b$  is given by

$$\mathcal{P}_b = \frac{\kappa_b}{R^5} \begin{pmatrix} R^2 - 3X_b^2 & -3X_b Y_b & -3X_b Z_b \\ -3X_b Y_b & R^2 - 3Y_b^2 & -3Y_b Z_b \\ -3X_b Z_b & -3Y_b Z_b & R^2 - 3Z_b^2 \end{pmatrix} - \begin{pmatrix} \Omega & 0 & 0 \\ 0 & \Omega & 0 \\ 0 & 0 & 0 \end{pmatrix}. \quad (24)$$

The corresponding velocity field (for QG flow) is given by

$$\begin{aligned} \mathbf{u}_b &= (-\partial/\partial y, \partial/\partial x, 0)\psi_b \\ &= \mathcal{L}\mathcal{P}_b \mathbf{x} + O(\kappa_b |\mathbf{x}|^2/R^4) \end{aligned} \quad (25)$$

from which it follows that  $\mathcal{S}_b = \mathcal{L}\mathcal{P}_b$  (cf. (1)). (Note,  $\mathcal{L}$  here is specific to QG flow; in general it gives the relation between velocity and streamfunction, i.e.  $\mathbf{u} = \mathcal{L}\nabla\psi$ .) Thus, in QG flow,

$$\mathcal{S}_b = \gamma \begin{pmatrix} 3\tilde{X}\tilde{Y} & 3\tilde{Y}^2 - 1 + \beta & 3\tilde{Y}\tilde{Z} \\ 1 - \beta - 3\tilde{X}^2 & -3\tilde{X}\tilde{Y} & -3\tilde{X}\tilde{Z} \\ 0 & 0 & 0 \end{pmatrix}, \quad (26)$$

where  $\tilde{X} \equiv X_b/R$ ,

$$\gamma \equiv \kappa_b/R^3, \quad (27)$$

hereinafter referred to as ‘the strain rate’, and

$$\beta \equiv \Omega/\gamma = (\kappa_b + \kappa_v)/\kappa_b \quad (28)$$

is a parameter depending only the ratio of the vortex strengths.

This form for the background flow matrix was considered by Meacham *et al.* (1994) and in subsequent works but using a different notation. It can be simplified further by choosing either  $\tilde{X}$  or  $\tilde{Y}$  to be zero, leaving only three non-zero components. For example, if  $\tilde{X} = 0$

$$\mathcal{S}_b = \gamma \begin{pmatrix} 0 & \frac{1}{2}(1 + 3 \cos 2\theta) + \beta & \frac{3}{2} \sin 2\theta \\ 1 - \beta & 0 & 0 \\ 0 & 0 & 0 \end{pmatrix}, \quad (29)$$

where  $\tilde{Z} = \sin \theta$  and  $\tilde{Y} = \cos \theta$ .

Note that even in this simplest case, there are three basic parameters describing the background flow:  $\gamma$ ,  $\beta$  and  $\theta$ . We present here a few examples to give a taste of what may be expected (a full exploration of the parameter space is the subject of current research). We consider two cross-sections through parameter space, in which only one parameter is varied. In the first, we fix  $\theta = 30^\circ$  and  $\gamma = Q/81$ , and take the vortex to be initially spherical. This seemingly small value of strain corresponds to that induced by an identical vortex only three radii distant, cf. (27). Figure 2 shows the evolution of the vortex when  $\beta = 2$  (then the background flow approximates that due to another vortex of the same circulation, cf. (28)). Initially, at time  $t = 0$ , the vortex semi-axes are aligned with the  $x$ -,  $y$ - and  $z$ -axes and the vortex rotates about the vertical. If no background flow is applied the vortex would retain its initial spherical shape and its orientation. However the instant application of the background flow causes the vortex to immediately undergo deformation of shape and a rapid rotation which leaves it tilted with respect to the vertical axis, as can be seen in figure 2 for time  $t = 10$ . We emphasize, however, that the matrix  $\mathcal{B}$  varies smoothly in time; the rapid changes in orientation occur when two axes become of equal length at one instant of time; afterwards, the axes switch since  $\hat{\mathbf{a}}$ ,  $\hat{\mathbf{b}}$  and  $\hat{\mathbf{c}}$  are always chosen so that  $a \leq b \leq c$ . The vortex then slowly precesses about the vertical axis. Between time  $t = 50$  and  $t = 60$  the vortex again undergoes a quick change in orientation when two of the axes exchange. This is followed by a similar event near time  $t = 120$ , when the vortex shape comes close to spherical. Figure 3 summarizes the results of various simulations having a range of  $\beta$  values. Here, the evolution of two measures of the departure from sphericity,  $\mathcal{B}_{11} - \bar{r}^2$  and  $\mathcal{B}_{22} - \bar{r}^2$ , where  $\bar{r}^3 = abc$  is the mean vortex radius, is shown for four different values of  $\beta$  in the various panels. The vortex is spherical only when these quantities are simultaneously zero. Note that the vortex returns to



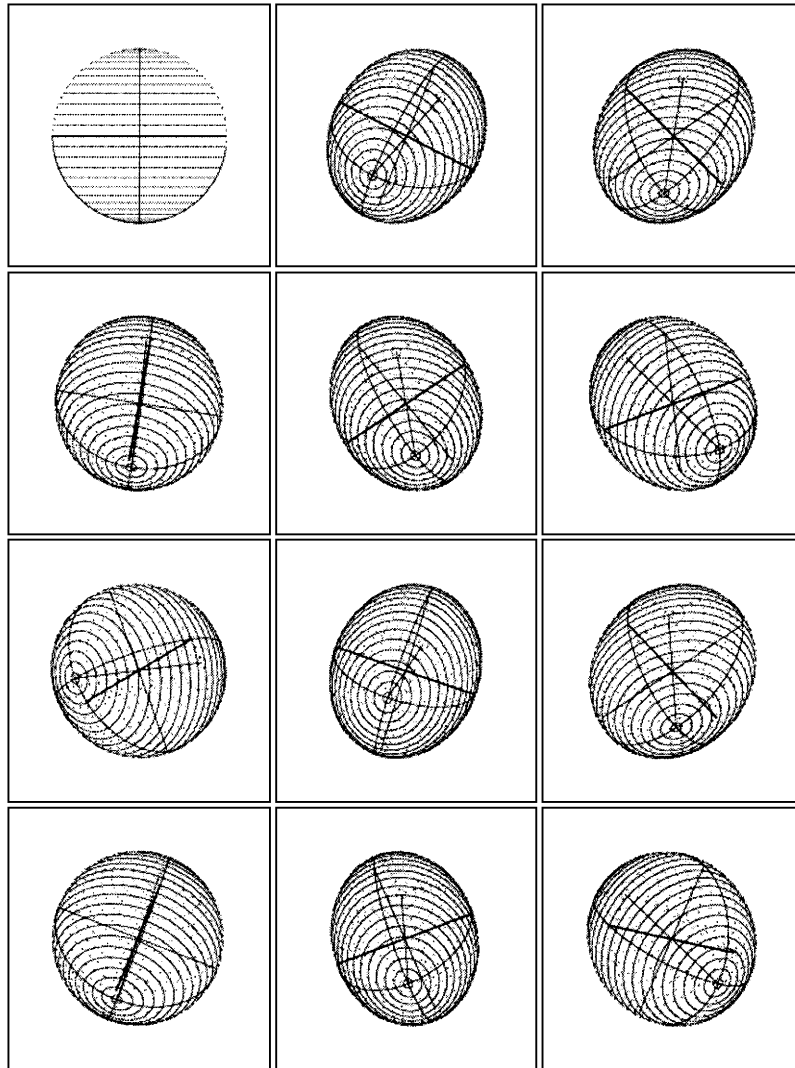


FIGURE 2. Evolution of an ellipsoid in a background flow characterized by  $\beta = 2$ ,  $\theta = 30^\circ$  and  $\gamma = Q/81$ . Time proceeds to the right and downwards starting from  $t = 0$  (when the vortex is spherical); the time interval between displayed images is 10. The co-latitude and longitude of the view are  $90^\circ$  and  $0^\circ$  (corresponding to a projection of the three-dimensional image onto the  $(y, z)$ -plane; from this perspective, one can observe that the height of the vortex is conserved). Ellipses are drawn in planes perpendicular to the major axis of the ellipsoid (indicated as a thin line). The front facing part of the ellipsoid is rendered with solid lines, while the back facing part is rendered with dashed lines. The minor axis is indicated as a bold line, while the intermediate axis is indicated as a thin line (in the plane of the equatorial ellipse).

a near spherical form occasionally. The oscillations seen lengthen with increasing  $\beta$ , and exhibit a change of character when  $\beta = 4$ . In all cases, the oscillations resemble a superposition of many waves of differing periods. However, on a much longer time scale (roughly 500 units of time) the oscillations appear to be periodic—see figure 4.

In the second cross-section, we fix  $\beta = 2$  and  $\gamma = Q/81$ , and again take the vortex to be initially spherical. Figure 5, like figure 3 previously, shows the evolution of the departures from sphericity for a range of angles  $\theta$ . The oscillation is again nearly

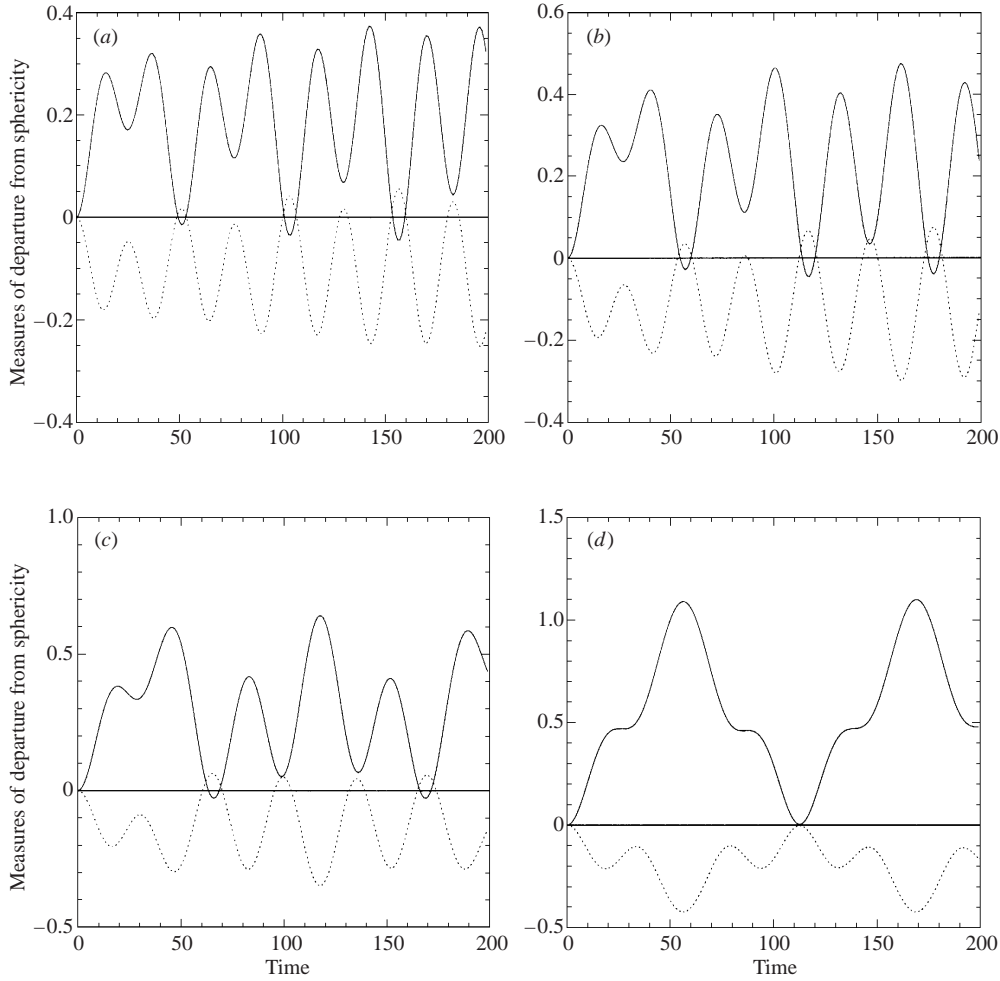


FIGURE 3. Evolution of parameters which measure the departure of the vortex shape from sphericity for  $\theta = 30^\circ$ ,  $\gamma = Q/81$  and for (a)  $\beta = 1$ , (b)  $\beta = 2$ , (c)  $\beta = 3$ , (d)  $\beta = 4$ . The solid curve is  $\mathcal{B}_{22} - \bar{r}^2$  and the dotted curve is  $\mathcal{B}_{11} - \bar{r}^2$ , where  $\bar{r}^3 = abc$  is the mean vortex radius (note that  $\mathcal{B}_{33}$  is a constant).

regular, particularly for  $\theta = 0$  (corresponding to a distant vortex centred on the same horizontal plane). As  $\theta \rightarrow 90^\circ$ , the amplitude of the oscillation tends to zero. This angle corresponds to a distant vortex located directly above the vortex, and in this configuration it cannot deform the vortex (the background flow matrix  $\mathcal{S}_b$  in (29) reduces to a pure rotation). Again, like in the previous series, all examples shown here are periodic on a sufficiently long time scale (not shown).

### 3.2. Vortex motion in a slowly varying background flow

The implicit assumption made in the previous subsection that the background flow is steady is not in general realistic. In a flow containing many vortices, such as QG turbulence, vortices drift together and apart under the influences of the vortices around them. The distance between vortex centres typically varies in time, and therefore the strain rate and rotation rate, as well as the angle  $\theta$  above, vary. The theory presented above in fact applies under these circumstances as well, since only the

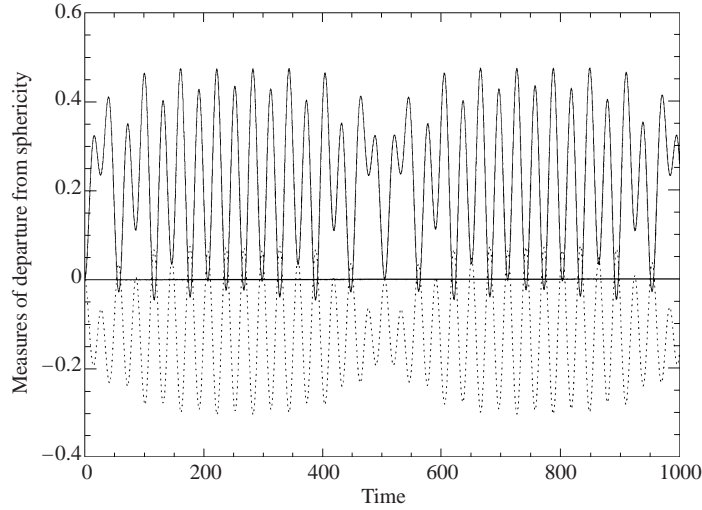


FIGURE 4. Extended evolution of  $\mathcal{B}_{11} - \bar{r}^2$  and  $\mathcal{B}_{22} - \bar{r}^2$  for  $\beta = 2$ ,  $\theta = 30^\circ$  and  $\gamma = Q/81$  showing the long-time periodic behaviour of the vortex motion.

instantaneous background flow is important in the evolution equation for the ellipsoid. In this subsection, we consider the effect of a slowly varying, weak background flow, arguably typical of the flow felt by vortices in dilute turbulence, when vortices are on average widely separated (cf. Dritschel, de la Torre Juárez & Ambaum 1999; Dritschel 1999). Of course, we cannot hope to describe strong interactions like merger, but these interactions are rare compared to the weak long-range interactions considered next.

For distant interactions, it is appropriate to assume that the dimensionless strain rate  $\epsilon = \gamma/Q \ll 1$  and moreover that the background flow varies on the long time scale  $\tau = \epsilon t$ . The flow matrix then takes the form

$$\mathcal{S}_b = \epsilon \mathcal{G}(\tau), \quad (30)$$

where  $\mathcal{G}$  is a matrix with five independent components like  $\mathcal{S}_b$  in (11). The matrix  $\mathcal{G}$ , and a sufficient number of time derivatives of  $\mathcal{G}$ , are assumed to be continuous. We furthermore assume that the vortex itself is slowly varying (on the long time  $\tau$ ) and that its shape departs by  $O(\epsilon)$  from an ellipsoid orientated with the  $x$ -,  $y$ - and  $z$ -axes, and having corresponding half-lengths  $p^{1/2}$ ,  $p^{1/2}$  and  $p^{-1}$ . This corresponds to a vortex of unit mean radius. This special choice of the basic vortex shape is made to prevent the ellipsoid from exhibiting fast time dependence (on  $t$ ) through self-rotation. Hence, we take

$$\mathcal{B}(\tau) = \mathcal{B}_0 + \epsilon \mathcal{B}_1(\tau) + \epsilon^2 \mathcal{B}_2(\tau) + O(\epsilon^3), \quad (31)$$

where  $\mathcal{B}_0$  is a diagonal matrix with the entries  $p$ ,  $p$  and  $p^{-2}$  down the diagonal. Since  $\mathcal{B}$  is a symmetric matrix, it has only six independent components, and it is convenient at this stage to introduce the following short-hand notation for the elements of  $\mathcal{B}$ :

$$\mathcal{B} = \begin{pmatrix} B^1 & B^2 & B^3 \\ B^2 & B^4 & B^5 \\ B^3 & B^5 & B^6 \end{pmatrix} = \sum_{k=1}^6 \mathcal{J}^k B^k, \quad (32)$$

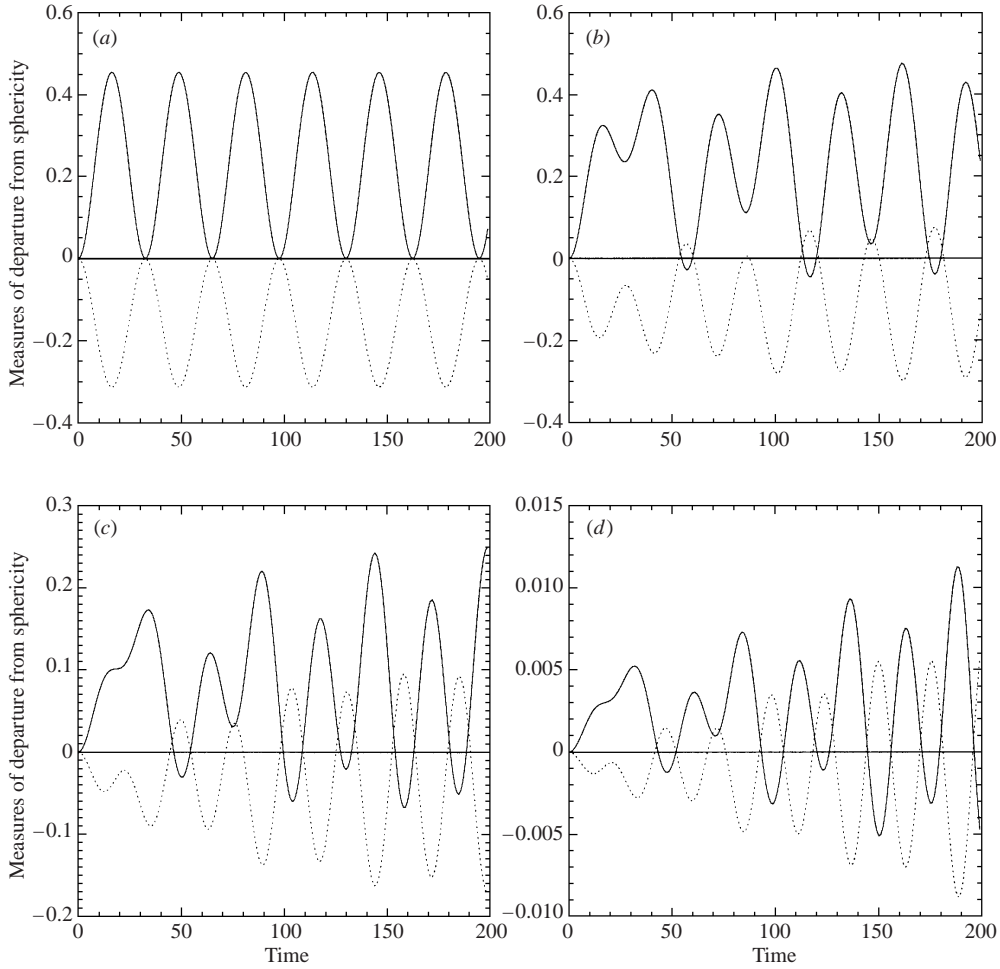


FIGURE 5. As figure 3, but with the fixed background flow parameters  $\beta = 2$ ,  $\gamma = Q/81$ , and for (a)  $\theta = 0^\circ$ , (b)  $\theta = 30^\circ$ , (c)  $\theta = 60^\circ$ , (d)  $\theta = 85^\circ$ .

where the matrices  $\mathcal{J}^k$  are

$$\left. \begin{aligned} \mathcal{J}^1 &= \begin{pmatrix} 1 & 0 & 0 \\ 0 & 0 & 0 \\ 0 & 0 & 0 \end{pmatrix}, & \mathcal{J}^2 &= \begin{pmatrix} 0 & 1 & 0 \\ 1 & 0 & 0 \\ 0 & 0 & 0 \end{pmatrix}, & \mathcal{J}^3 &= \begin{pmatrix} 0 & 0 & 1 \\ 0 & 0 & 0 \\ 1 & 0 & 0 \end{pmatrix}, \\ \mathcal{J}^4 &= \begin{pmatrix} 0 & 0 & 0 \\ 0 & 1 & 0 \\ 0 & 0 & 0 \end{pmatrix}, & \mathcal{J}^5 &= \begin{pmatrix} 0 & 0 & 0 \\ 0 & 0 & 1 \\ 0 & 1 & 0 \end{pmatrix}, & \mathcal{J}^6 &= \begin{pmatrix} 0 & 0 & 0 \\ 0 & 0 & 0 \\ 0 & 0 & 1 \end{pmatrix}. \end{aligned} \right\} \quad (33)$$

This expansion (equation (31)) is constrained by conservation of vortex height and volume, equivalent to  $B^6 = \text{constant}$  and  $|\mathcal{B}| = \text{constant}$ . The first constraint implies that  $B_0^6 = p^{-2}$  and  $B_n^6 = 0$  for orders  $n > 0$ . The second constraint implies at  $O(\epsilon^1)$

$$B_1^4 = -B_1^1 \quad (34)$$

and at  $O(\epsilon^2)$

$$B_2^1 + B_2^4 = p^2[(B_1^3)^2 + (B_1^5)^2] + \frac{1}{p}[(B_1^1)^2 + (B_1^2)^2]. \quad (35)$$

Next, using the evolution equation (18) for  $\mathcal{B}$ , we have

$$\begin{aligned} \epsilon^2 \frac{d\mathcal{B}_1}{d\tau} + O(\epsilon^3) &= (\mathcal{B}_0 + \epsilon\mathcal{B}_1 + \epsilon^2\mathcal{B}_2 + \cdots)[\mathcal{S}_v^T(\mathcal{B}_0 + \epsilon\mathcal{B}_1 + \epsilon^2\mathcal{B}_2 + \cdots) + \epsilon\mathcal{G}^T] \\ &+ [\mathcal{S}_v(\mathcal{B}_0 + \epsilon\mathcal{B}_1 + \epsilon^2\mathcal{B}_2 + \cdots) + \epsilon\mathcal{G}](\mathcal{B}_0 + \epsilon\mathcal{B}_1 + \epsilon^2\mathcal{B}_2 + \cdots). \end{aligned} \quad (36)$$

*Zeroth order:*

At  $O(\epsilon^0)$ , equation (36) gives

$$\mathcal{B}_0\mathcal{S}_v^T(\mathcal{B}_0) + \mathcal{S}_v(\mathcal{B}_0)\mathcal{B}_0 = 0, \quad (37)$$

which is always satisfied for the diagonal form of  $\mathcal{B}_0$  taken. Here,  $\mathcal{S}_v = \mathcal{L}\mathcal{F}$  where  $\mathcal{F}$  is given by (13) and (14) with  $\xi_a = \xi_b = \frac{1}{3}R_D(p, p^{-2}, p)$  (cf. (15)), or explicitly

$$\mathcal{S}_v(\mathcal{B}_0) = \begin{pmatrix} 0 & -\xi_a & 0 \\ \xi_a & 0 & 0 \\ 0 & 0 & 0 \end{pmatrix}, \quad (38)$$

where we have taken  $Q = 1$  without loss of generality to simplify  $\kappa_v = \frac{1}{3}Qabc \rightarrow \frac{1}{3}$ .

*First order:*

At  $O(\epsilon^1)$ , equation (36) gives

$$\sum_{k=1}^5 \mathcal{C}^k B_1^k = \mathcal{H}_1, \quad (39)$$

where

$$\begin{aligned} \mathcal{C}^k &= \frac{\partial}{\partial B^k} [\mathcal{B}_0\mathcal{S}_v^T(\mathcal{B}) + \mathcal{B}\mathcal{S}_v^T(\mathcal{B}_0) + \mathcal{S}_v(\mathcal{B})\mathcal{B}_0 + \mathcal{S}_v(\mathcal{B}_0)\mathcal{B}] \Big|_{\mathcal{B}=\mathcal{B}_0} \\ &= \frac{\partial \mathcal{S}_v}{\partial B^k} \Big|_{\mathcal{B}=\mathcal{B}_0} \mathcal{B}_0 + \mathcal{S}_v(\mathcal{B}_0)\mathcal{J}^k + \mathcal{J}^k\mathcal{S}_v^T(\mathcal{B}_0) + \mathcal{B}_0 \frac{\partial \mathcal{S}_v^T}{\partial B^k} \Big|_{\mathcal{B}=\mathcal{B}_0} \end{aligned} \quad (40a)$$

$$\mathcal{H}_1 = -(\mathcal{B}_0\mathcal{G}^T + \mathcal{G}\mathcal{B}_0). \quad (40b)$$

The matrices  $\mathcal{C}^k$  have the forms

$$\mathcal{C}^1 = -\mathcal{C}^4 = e_1\mathcal{J}^2, \quad \mathcal{C}^2 = 2e_1(\mathcal{J}^4 - \mathcal{J}^1), \quad \mathcal{C}^3 = e_2\mathcal{J}^5, \quad \mathcal{C}^5 = -e_2\mathcal{J}^3, \quad (41)$$

where  $e_1(p)$  and  $e_2(p)$  involve elliptic integrals and are plotted in figure 6 versus  $p$ .

Note in particular that the product of  $\mathcal{C}^k$  and  $\mathcal{C}^j$  element-wise, denoted  $\mathcal{C}^k \otimes \mathcal{C}^j$ , is zero if  $j \neq k$  (excluding  $k$  or  $j = 4$ ). Hence, we can directly solve for the  $B_1^k$  in (39) by applying  $\mathcal{C}^i \otimes$  to both sides of the equation, yielding

$$B_1^1 - B_1^4 = \frac{\mathcal{C}^1 \otimes \mathcal{H}_1}{2e_1^2}, \quad B_1^2 = \frac{\mathcal{C}^2 \otimes \mathcal{H}_1}{8e_1^2}, \quad B_1^3 = \frac{\mathcal{C}^3 \otimes \mathcal{H}_1}{2e_2^2}, \quad B_1^5 = \frac{\mathcal{C}^5 \otimes \mathcal{H}_1}{2e_2^2}, \quad (42)$$

together with the volume constraint  $B_1^4 = -B_1^1$ .

Second order:

At  $O(\epsilon^2)$ , equation (36) gives

$$\sum_{k=1}^5 \mathcal{C}^k B_2^k = \mathcal{H}_2, \quad (43)$$

where

$$\mathcal{H}_2 = \frac{d\mathcal{B}_1}{d\tau} - (\mathcal{B}_1 \mathcal{G}^T + \mathcal{G} \mathcal{B}_1) - \sum_{m=1}^5 \sum_{n=1}^5 \mathcal{H}^{mn} B_1^m B_1^n, \quad (44a)$$

$$\mathcal{H}^{mn} = \frac{1}{2} \frac{\partial^2 \mathcal{P}_v}{\partial B^m \partial B^n} \Big|_{\mathcal{B}=\mathcal{B}_0} \mathcal{B}_0 + \frac{\partial \mathcal{P}_v}{\partial B^m} \Big|_{\mathcal{B}=\mathcal{B}_0} \mathcal{J}^n + \mathcal{J}^n \frac{\partial \mathcal{P}_v^T}{\partial B^m} \Big|_{\mathcal{B}=\mathcal{B}_0} + \mathcal{B}_0 \frac{1}{2} \frac{\partial^2 \mathcal{P}_v^T}{\partial B^m \partial B^n} \Big|_{\mathcal{B}=\mathcal{B}_0}, \quad (44b)$$

and where the  $5 \times 5$  ‘matrix of matrices’  $\mathcal{H}$  is

$$\begin{pmatrix} d_1 \mathcal{J}^2 & d_6 \mathcal{J}^1 + d_7 \mathcal{J}^4 & d_8 \mathcal{J}^5 & d_2 \mathcal{J}^2 & d_9 \mathcal{J}^3 \\ d_{10} \mathcal{J}^1 + d_3 \mathcal{J}^4 & 0 & d_{11} \mathcal{J}^3 & -d_3 \mathcal{J}^1 - d_{10} \mathcal{J}^4 & -d_{11} \mathcal{J}^5 \\ d_4 \mathcal{J}^5 & d_{12} \mathcal{J}^3 & d_{13} \mathcal{J}^2 & d_{14} \mathcal{J}^5 & d_5 \mathcal{J}^1 + d_{15} \mathcal{J}^4 \\ -d_2 \mathcal{J}^2 & -d_7 \mathcal{J}^1 - d_6 \mathcal{J}^4 & -d_9 \mathcal{J}^5 & -d_1 \mathcal{J}^2 & -d_8 \mathcal{J}^3 \\ -d_{14} \mathcal{J}^3 & -d_{12} \mathcal{J}^5 & -d_{15} \mathcal{J}^1 - d_5 \mathcal{J}^4 & -d_4 \mathcal{J}^3 & -d_{13} \mathcal{J}^2 \end{pmatrix}. \quad (45)$$

There appear to be five independent coefficients  $d_k$ ; we have found the following ten relations among these coefficients:

$$d_6 = 2d_2 - d_3, \quad (46a)$$

$$d_7 = 2d_1 - d_3, \quad (46b)$$

$$d_8 = d_1 - d_3 + d_4, \quad (46c)$$

$$d_9 = -\frac{3d_1 + d_2 + d_3}{2} - d_4, \quad (46d)$$

$$d_{10} = d_3 - 2(d_1 + d_2), \quad (46e)$$

$$d_{11} = \frac{d_1 + d_2 + 3d_3}{2}, \quad (46f)$$

$$d_{12} = \frac{3(d_1 + d_2) + d_3}{2}, \quad (46g)$$

$$d_{13} = -2(d_1 + d_2 + d_3), \quad (46h)$$

$$d_{14} = \frac{3(d_1 + d_2) + d_3}{2} + d_4, \quad (46i)$$

$$d_{15} = d_5 - 4(d_1 + d_2 + d_3); \quad (46j)$$

see figure 7 for the dependence of the  $d_k$ ,  $k = 1, 2, \dots, 5$ , on the vortex shape  $p$ .

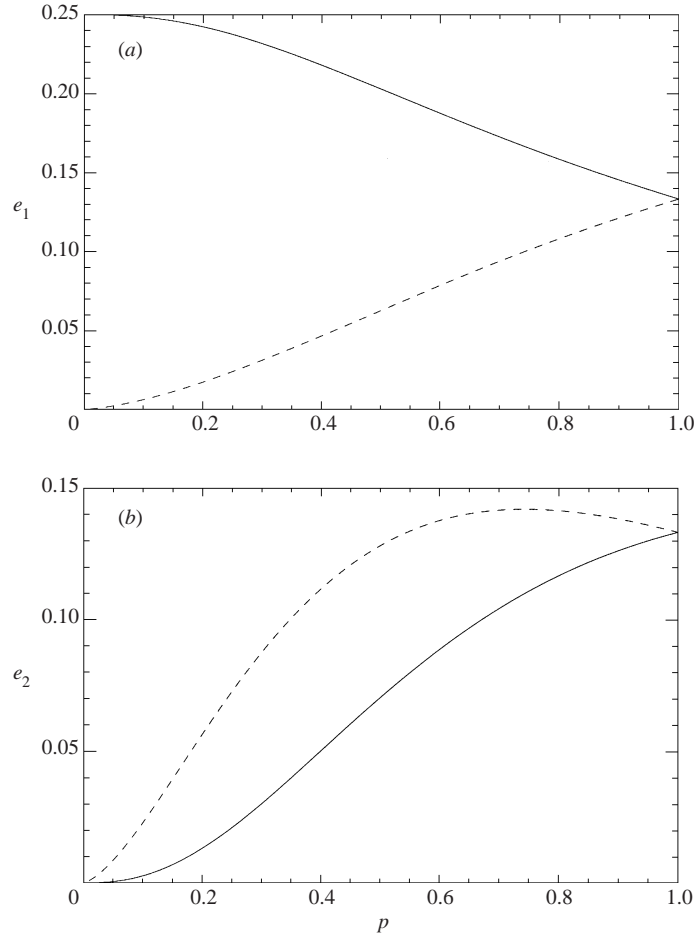


FIGURE 6. The dependence of the first-order coefficients  $e_1$  (a) and  $e_2$  (b) on the vortex shape  $p$  and its inverses  $1/p$ . The solid curves correspond to the coefficients as a function of  $p$  for values of  $p \leq 1$ , and the dashed curve corresponds to the coefficients as a function of  $1/p$  for values of  $p > 1$ .

Taking the element-wise product of the  $\mathcal{C}^k$  matrices with (43) gives

$$B_2^1 - B_2^4 = \frac{\mathcal{C}^1 \otimes \mathcal{H}_2}{2e_1^2}, \quad B_2^2 = \frac{\mathcal{C}^2 \otimes \mathcal{H}_2}{8e_1^2}, \quad B_2^3 = \frac{\mathcal{C}^3 \otimes \mathcal{H}_2}{2e_2^2}, \quad B_2^5 = \frac{\mathcal{C}^5 \otimes \mathcal{H}_2}{2e_2^2}, \quad (47)$$

and the volume constraint (35) allows one to determine  $B_2^1$  and  $B_2^4$  separately in terms of the  $B_1^k$ .

Note that these matrix elements  $B_2^k$  depend on the slow time variation of  $\mathcal{B}_1$  through the  $d\mathcal{B}_1/d\tau$  term in  $\mathcal{H}_2$ , cf. (44a). Thus, since the elements  $B_1^k$  depend on the slowly varying background flow matrix  $\mathcal{G}(\tau)$  through (40b) and (42), then the  $B_2^k$  actually involve the *rate of change* of the background flow matrix.

These solutions describe the slow evolution of the ellipsoid in a weak, slowly varying background flow, to second order in the strain rate, and in the rate of change of the background flow. Note that to first order, the vortex evolves adiabatically by adopting an instantaneous equilibrium with the background flow. At second order, the vortex departs slightly from this equilibrium but still evolves on the long time scale  $\tau = \epsilon t$ . This quasi-adiabatic evolution has been observed frequently in two-

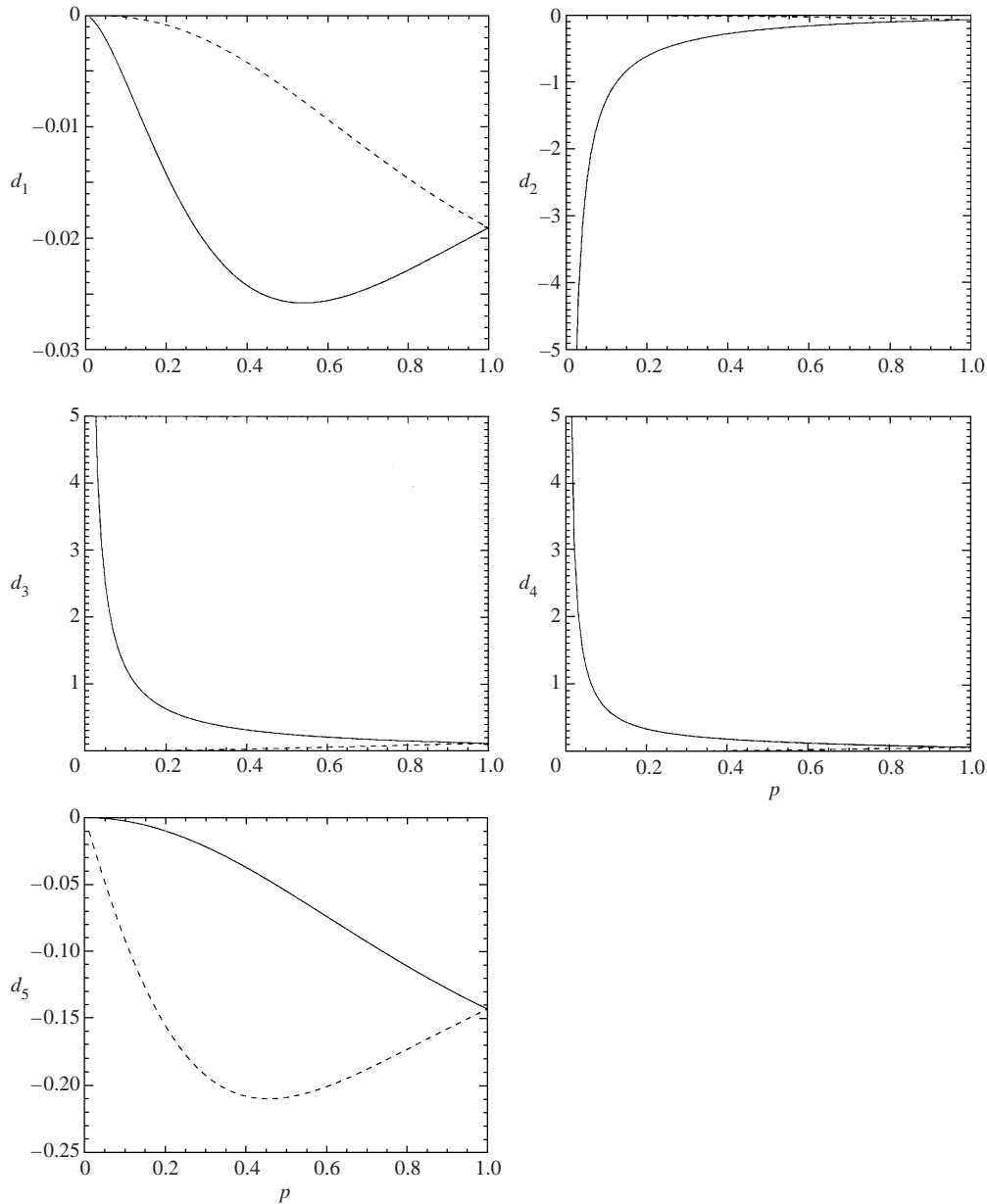


FIGURE 7. The dependence of the second-order coefficients  $d_1, d_2, \dots$ , and  $d_5$  on the vortex shape  $p$  and its inverse  $1/p$ . The solid curves correspond to the coefficients as a function of  $p$  for values of  $p \leq 1$ , and the dashed curve corresponds to the coefficients as a function of  $1/p$  for values of  $p > 1$ .

dimensional vortex dynamics (Dritschel 1995; Legras, Dritschel & Caillol 2001), but it appears to be far more general. Slow evolution appears possible for any slowly forced dynamical system so long as the nearby equilibrium is a stable one.

We examine next several examples, using three values of the vortex shape parameter  $p = \frac{1}{2}, 1$  and  $2$ , to see how well the theory presented above compares with integrations of the exact equations of motion for an ellipsoid. For simplicity, we take  $\mathcal{G}(\tau) = g(\tau)\mathcal{V}$  here, where  $\mathcal{V}$  is a constant matrix of the form given in (29) with  $\beta = 2$  and  $\theta = 30^\circ$ .



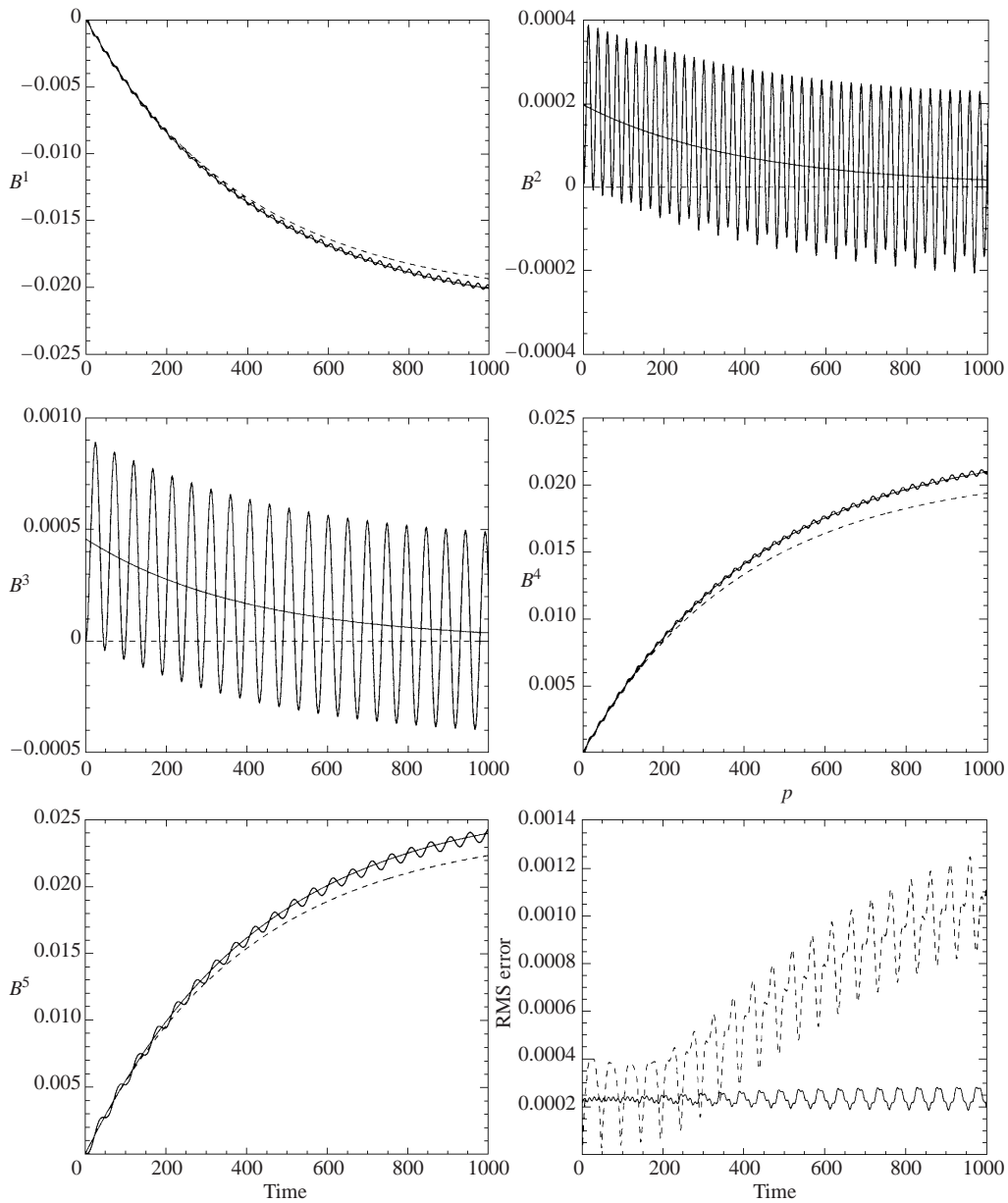


FIGURE 8. The evolution of  $B^k$ ,  $k = 1, 2, \dots, 5$  from  $t = 0$  to 1000, for case (i). Here,  $\epsilon = 0.0025$ ,  $t_m = 400$ ,  $\beta = 2$ ,  $\theta = 30^\circ$ , and  $p = 1$ . The bold, dashed, and thin curves correspond to the full equations, the first-order theory, and the second-order theory, respectively. The r.m.s. errors of the first- and second-order theories are shown in the lower right frame.

Two cases are considered: (i)  $g(\tau) = 1 - \exp(-\tau/\tau_m)$  and (ii)  $g(\tau) = 1 - \exp(-(\tau/\tau_m)^2)$ . In case (i), the initial growth is linear in time, while in case (ii) it is quadratic.

The evolution of the  $B^k$  ( $k = 1-5$ ) is shown for case (i) in figure 8 and for case (ii) in figure 9, with the bold curves showing the results of the full equations, the dashed curves showing the first-order theory, and the thin solid curves showing the second-order theory. Also shown in the lower right-hand frame is the r.m.s. error

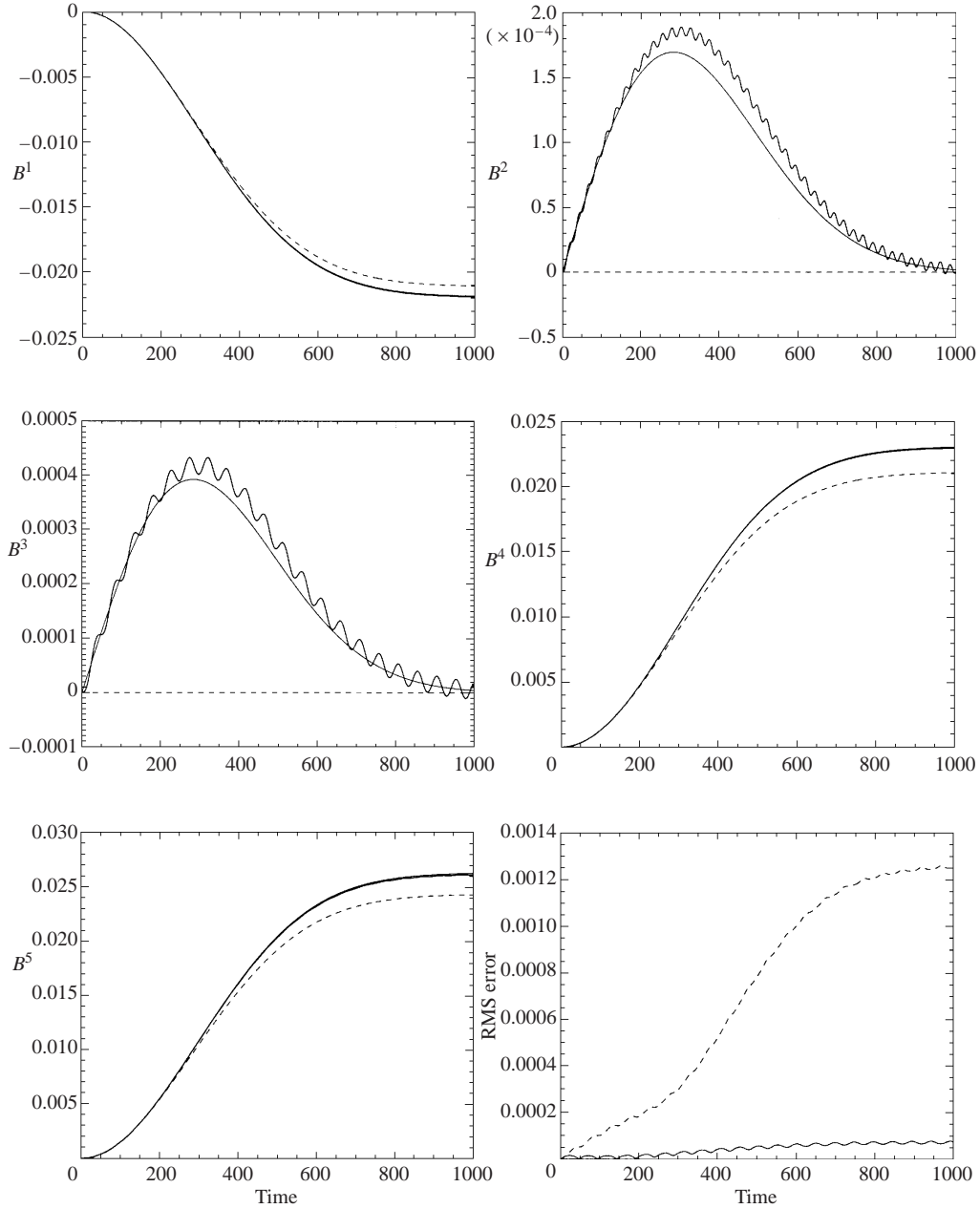


FIGURE 9. As figure 8, but for case (ii) ( $g(\tau) = 1 - \exp(-\tau/\tau_m)^2$ ).

$[\frac{1}{5} \sum_{k=1}^5 (B_{\text{approx}}^k - B^k)^2]^{1/2}$ . All of these results are for an initial vortex having  $p = 1$ . We have taken  $\epsilon = 0.0025$  and  $\tau_m = 1$ , corresponding to a strain growth period of  $t_m = \epsilon^{-1} = 400$ . This value of strain may seem small, but recall that the strain rate induced by a vortex falls off with the inverse cube of the distance from the vortex, cf. (27). For instance, given a background and target vortex of the same uniform PV, the background vortex would induce this value of strain when it is only  $(3\epsilon)^{-1/3}R \approx 5.1R$  distant from the centre of the target vortex, where  $R$  is the

mean radius of the background vortex. Doubling  $\epsilon$  reduces the above distance to approximately  $4R$ .

The results shown in figures 8 and 9 demonstrate that the second-order theory comes much closer to capturing the full dynamics than the first-order theory (note that  $B_1^2 = B_1^3 = 0$  for all time). The main discrepancy, particularly in case (i), is the failure to capture a relatively short-period oscillation (though note that its mean level is accurately predicted). This oscillation is due to the wobbling of the vortex about the quasi-adiabatic equilibrium, and also occurs for ellipses in two dimensions (Legras *et al.* 2001). It cannot be captured by the theory presented simply because the theory assumes a slow time dependence. However, note that the amplitude of the oscillation is an order of magnitude less in case (ii) than in case (i). In case (ii), the strain grows quadratically in time initially, and the weaker oscillation suggests that its origin lies in the initial conditions. That is, the oscillation can be potentially eliminated by a judicious choice of the initial conditions.

To see what is required, we need only apply the theory presented above at  $t = 0$ . We seek the corrections  $B_m^k$ ,  $m = 1, 2, \dots$ , to our original vortex  $B_0^k$  such that no fast oscillations are induced, order by order. We also insist that the corrections preserve the original volume and the height of the vortex ( $|\mathcal{B}|$  and  $B^6$  are left unchanged). The first- and second-order corrections are in fact given already in equations (42) and (47) (together with the volume constraints (34) and (35)). That is, we use the theory to second order in  $\epsilon$  to adjust the initial conditions used for the *exact* equations in order to reduce the subsequent oscillations. In the second case of initially quadratic strain growth in time, figure 9 shows that all of the corrections to  $\mathcal{B}_0$  are initially zero to second order. However, in case (i) (having initially linear strain growth), figure 8 shows that there is a non-zero correction to  $B^2$  and  $B^3$  initially. This stems from the term  $d\mathcal{B}_1/d\tau$  in  $\mathcal{H}_2$  at second order (cf. (44a)). This is the only non-zero term at  $\tau = 0$ , and it gives rise to non-zero values of  $B_2^2$  and  $B_2^3$ . For the second case, even this term is zero, and one may anticipate that third-order corrections to the initial conditions are necessary to reduce the small oscillations seen in figure 9 (though no attempt is made to go this far).

Let us then re-examine case (i), now using adjusted initial conditions for the exact equations. The results are shown in figure 10 (cf. figure 8). The much weaker oscillations observed here demonstrate that the oscillations are a product of the initial conditions. In theory, it appears possible to reduce these oscillations to arbitrarily small levels, leading to a completely slow evolution for the exact equations. In this case, the shape and orientation of the vortex are controlled by the background flow.

Other values of the initial vortex shape  $p$  give qualitatively similar results. Comparisons of the full equations, the first-order theory, and the second-order theory following the format of figures 8 and 9 for  $p = 1$  are given in figures 11 and 12 for  $p = \frac{1}{2}$  (for a prolate ellipsoid), and in figures 13 and 14 for  $p = 2$  (for an oblate ellipsoid). The pair of figures for each  $p$  correspond to the two cases of initially linear and quadratic strain growth. In case (i), we have used adjusted initial conditions for the full equations to reduce the short-time-scale oscillations, as just discussed. In case (ii), the largest deviation of the theory from the full equations occurs at the time when the rate of change of the strain growth is a maximum. This can be seen for  $B_2^2$  and  $B_2^3$  at approximately time  $t = 280$  in figures 9, 12 and 14. The results indicate that the theories are less accurate for prolate ellipsoids than they are for oblate ones, and apparently most accurate for nearly spherical vortices. This may be because the period of the (relatively) high-frequency oscillations is shorter for the nearly spherical vortices than for the oblate and prolate ellipsoids. This would indicate that the accu-

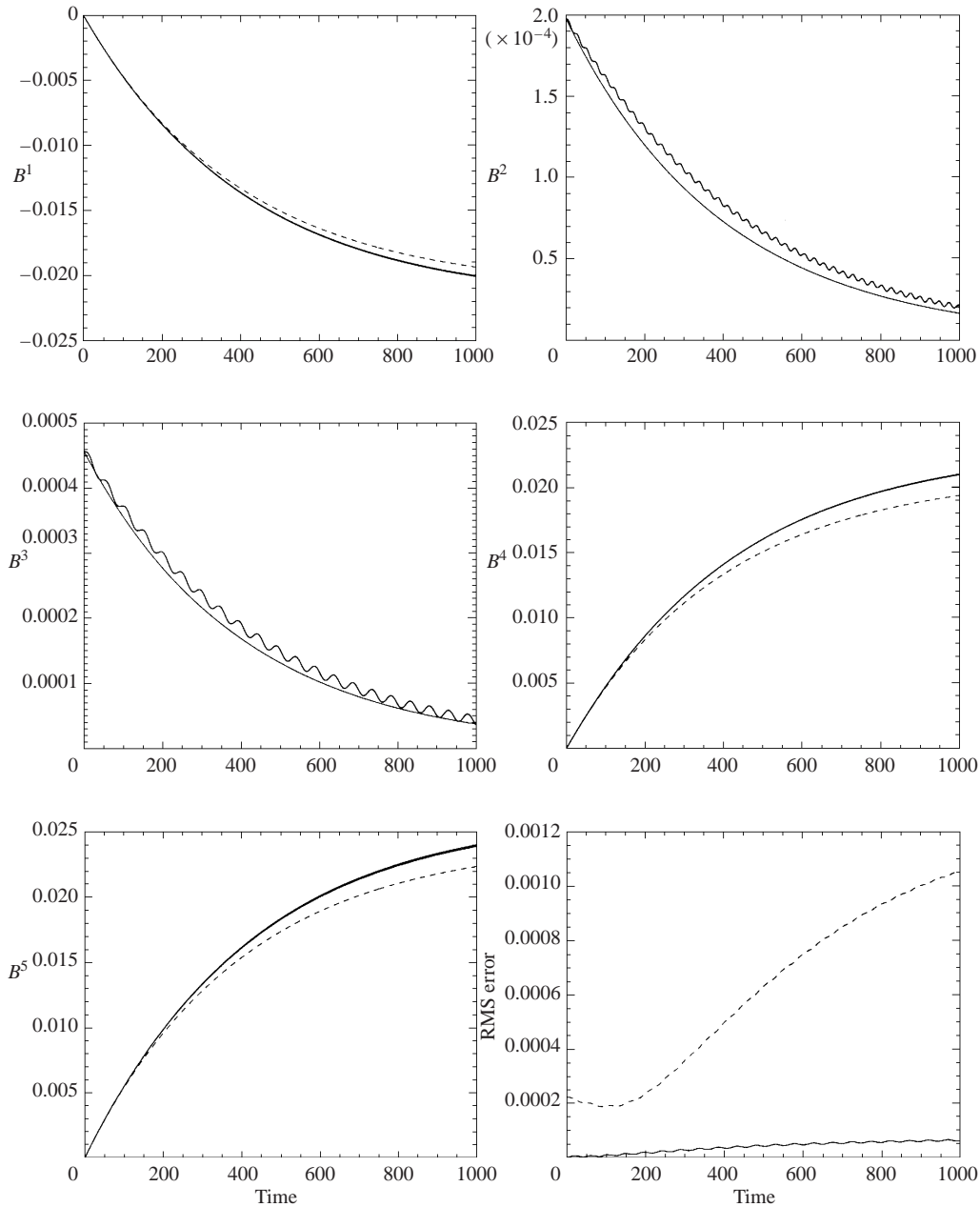


FIGURE 10. As in figure 8 for initially linear strain growth, but using adjusted initial conditions for the exact equations to reduce the subsequent oscillations. Note,  $B_1^2 = B_1^3 = 0$  for all time.

racy of the theories is better when the period of these high-frequency oscillations is shorter. Nevertheless, we have checked that the theories converge, at times  $t = O(t_m)$ , by varying both the maximum strain rate  $\epsilon$  and the strain growth period  $t_m$ . For  $1/t_m \sim \epsilon$ , the r.m.s. errors are  $O(\epsilon^2)$  and  $O(\epsilon^3)$  for the first- and second-order theories, respectively.

The above analysis may help to interpret the behaviour of vortices in more complex

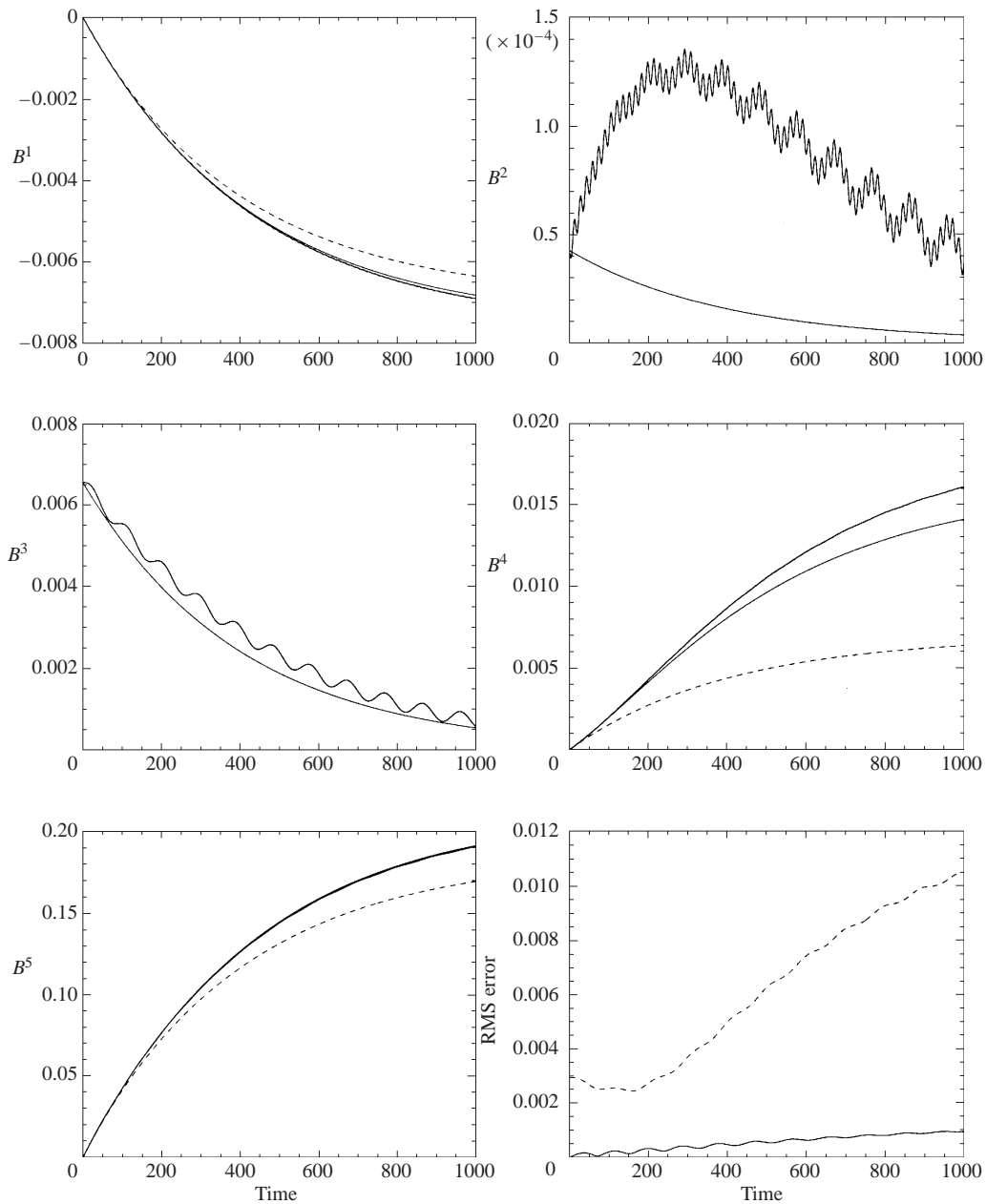


FIGURE 11. As in figure 8 featuring initially linear strain growth, but for  $p = 0.5$  (note, adjusted initial conditions are used for the exact equations). Note,  $B_1^2 = B_1^3 = 0$  for all time.

flows, such as rotating stratified (QG) turbulence. Could it be true that vortices interact quasi-adiabatically over most of their lifetimes? If so, many aspects of their interactions can be understood from the above analysis, which represents a great simplification of the full fluid equations. Then, this would mean that the dynamics of the flow may be reduced, mostly, to that of interacting ‘point’ vortices, albeit with a modified interaction law that depends on the shape and orientation (through the  $\mathcal{B}$  matrix)

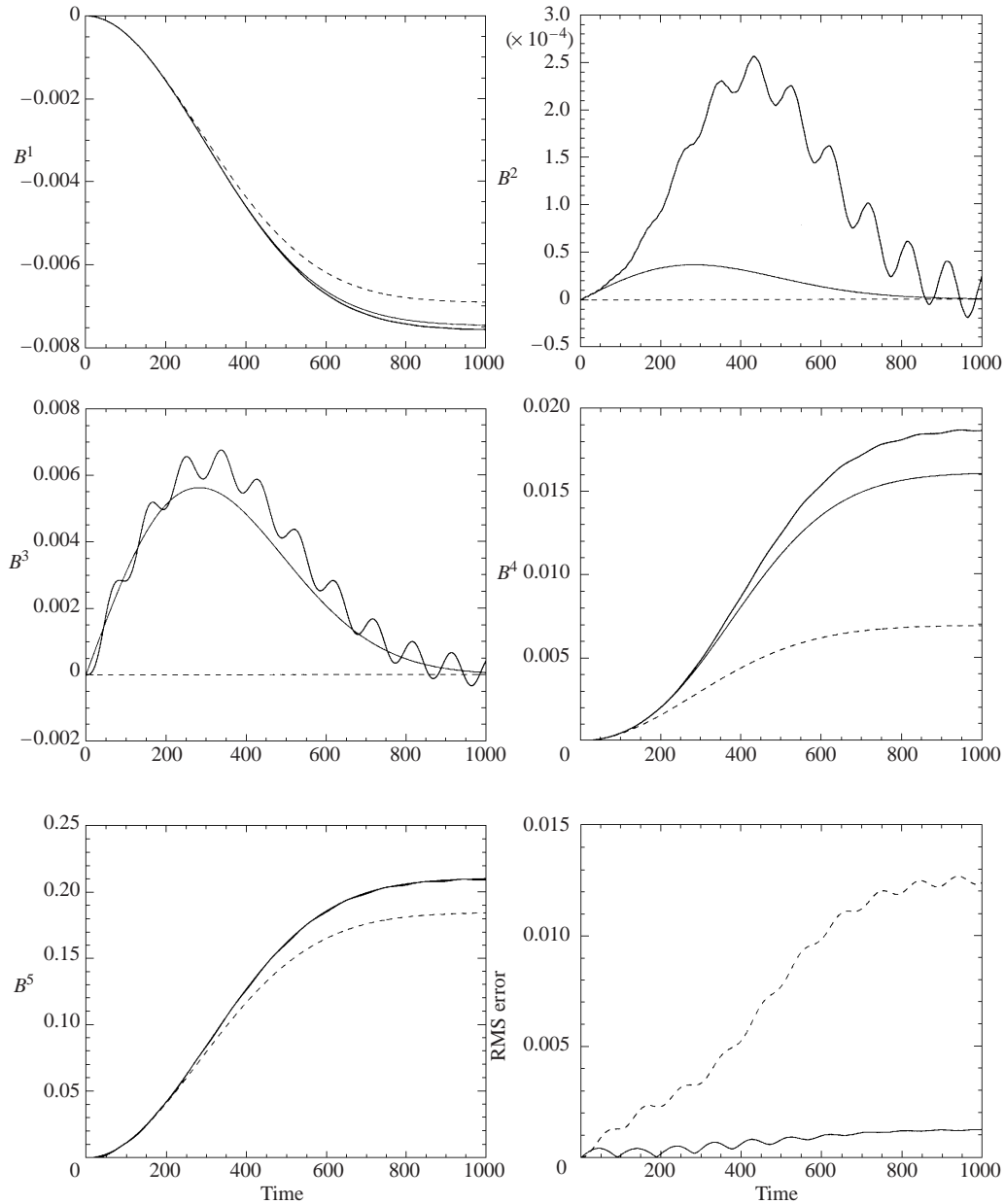


FIGURE 12. As figure 11 ( $p = 0.5$ ) but for case (ii) (initially quadratic strain growth).

of the vortices. There is support for this idea in two-dimensional flow (cf. Dritschel 1995; Legras *et al.* 2001). Current work on three-dimensional QG turbulence also suggests that this idea may hold there as well (Reinaud, Dritschel & Koudella 2003).

#### 4. Conclusions

We have shown that the equations governing the motion of a fluid ellipsoid in a linear background flow may be written simply in terms of two  $3 \times 3$  matrices

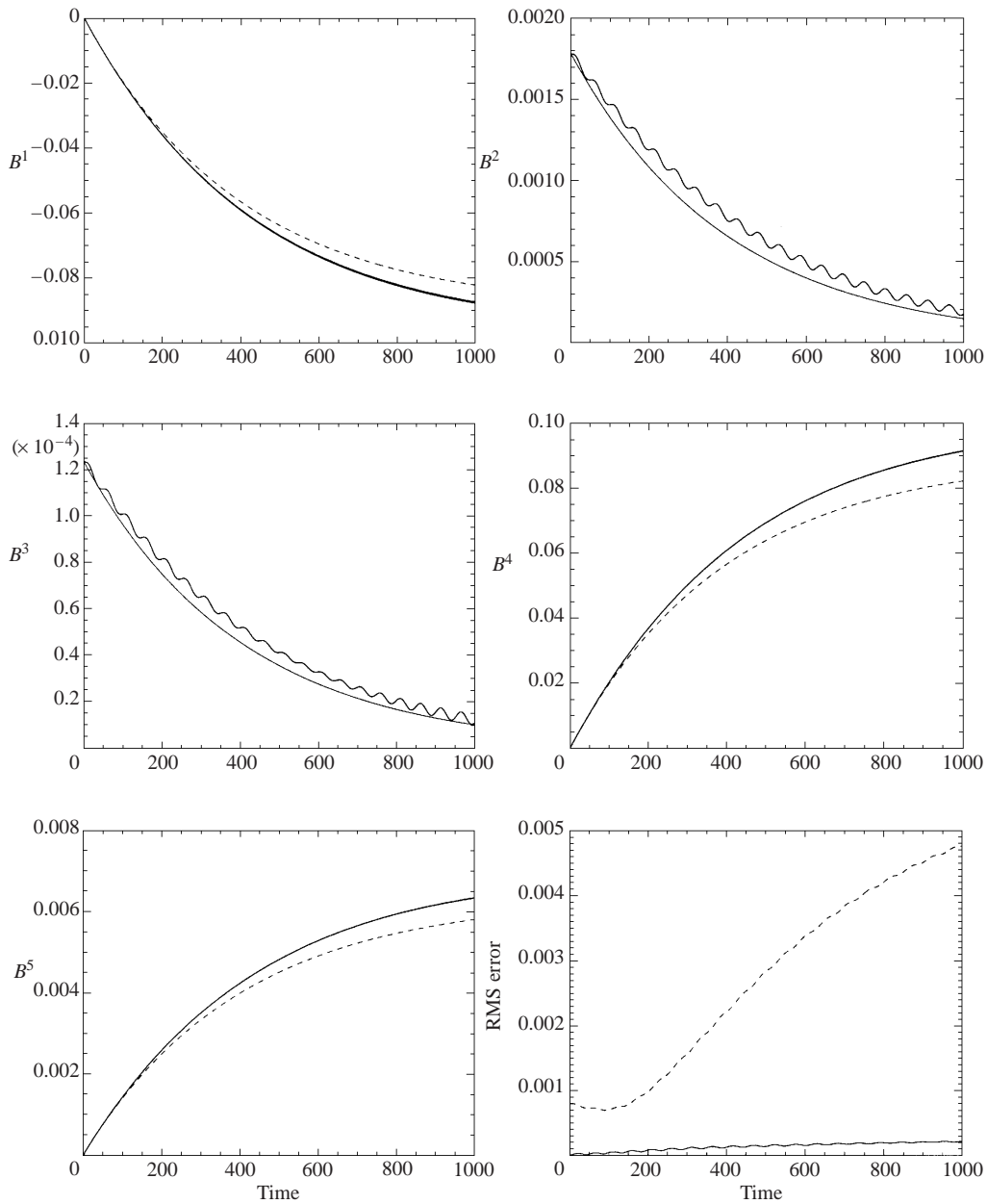


FIGURE 13. As in figure 8 featuring initially linear strain growth, but for  $p = 2$  (again, adjusted initial conditions are used for the exact equations). Note,  $B_1^2 = B_1^3 = 0$  for all time.

$\mathcal{B}$  and  $\mathcal{S}$ . The former symmetric matrix contains all the information necessary to describe the shape and orientation of an arbitrary ellipsoid. The latter matrix specifies the gradient of the velocity field at the edge of the ellipsoid. It consists of a self-induced part (originally calculated by Laplace in 1784) and a background part, representing the leading-order effects of distant vortices not explicitly modelled.

The advantage of this formulation over, say, one using orientation angles and axis lengths (Meacham *et al.* 1994) is that the equations are free from singularities.

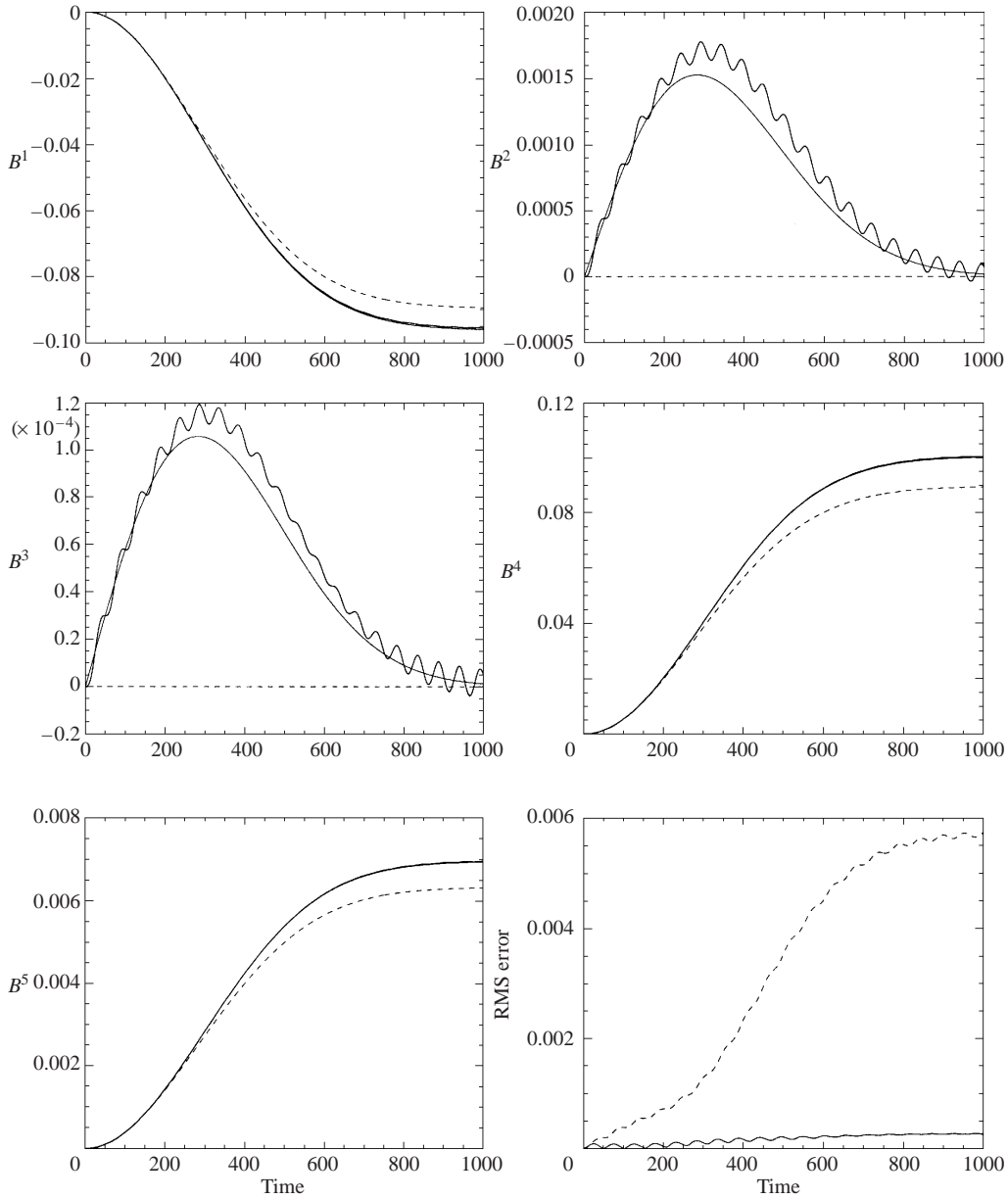


FIGURE 14. As figure 13 ( $p = 2$ ) but for case (ii) (initially quadratic strain growth).

To a degree, this formulation is not new: the elements of the  $\mathcal{B}$  matrix were used by Meacham *et al.* (1997) and later by Miyazaki and co-workers. However, they did not consider evolving the matrix directly via the remarkably simple equation  $d\mathcal{B}/dt = \mathcal{B}\mathcal{I}^T + \mathcal{I}\mathcal{B}$ , nor did they indicate how one can recover all of the shape characteristics of the vortex via the eigenproblem (21). We have also presented this model in a more general way so that it can be easily adapted for other applications (a code has been made available at <http://www-vortex.mcs.st-andrews.ac.uk>).

We have developed a theory for the slow, quasi-adiabatic evolution of a vortex in a



weak, slowly varying background flow. In this theory, the full shape and orientation of the vortex is controlled by the background flow. To first order in the dimensionless strain rate, the vortex adopts an instantaneous equilibrium with the background flow. To second order, the vortex departs slightly from this equilibrium, but in such a way as to allow it to slowly evolve from one near-equilibrium state to the next. It remains to be shown how frequent this behaviour is in flows containing many vortices, and whether or not vortices are attracted to this quasi-adiabatic state of evolution. That is, do their internal oscillations damp out? Evidence for this, in two-dimensional flows, is available in Legras *et al.* (2001).

It is tempting to construct a simplified model of many interacting vortices (as in QG turbulence) using ellipsoids. This would give a more accurate estimate of the background flow matrix  $\mathcal{S}_b$  as well as an equation for the evolution of the centroid of each vortex. This has in fact been done recently by Miyazaki *et al.* (2001), employing the full equations for each ellipsoid (no quasi-adiabatic assumption), and working out the leading-order flow induced by each ellipsoid on all others, as in §3.1 here. The limitation of this model, however, is that it parameterizes the merger of vortices in an *ad hoc* manner. The merger or close interaction of vortices is a highly complex process (cf. Dritschel 2002; Reinaud & Dritschel 2002). In particular, as in two dimensions (Dritschel & Waugh 1992; Dritschel & Zabusky 1996), vortex merger is a poor description of close vortex interactions. But the three-dimensional situation is further complicated by the fact that vortex interactions can often produce more vortices than there were to begin with. It is unlikely, in our opinion, that any parameterization of such interactions will be even qualitatively correct. The only recourse is to use a more complete set of equations (in which the ellipsoidal approximation is abandoned) under these circumstances. It may be possible to do this locally and over a short time interval thereby retaining much of the simplicity of the ellipsoidal model.

There are several ways in which this work can be usefully extended. First, a more complete account of the background flow due to surrounding vortices can be included by explicitly calculating the part of this background flow which preserves the ellipsoidal shape of a given vortex. This is not the same as using a Taylor series expansion, as done in §3.1 and by Miyazaki *et al.* (2001). The explicit calculation of the background flow was done by Legras & Dritschel (1991) in the two-dimensional ‘elliptical model’, and it was shown to be significantly more accurate in modelling close-range interactions than a series-based (or moment-based) approach (see also Dritschel & de la Torre Juárez 1996). For example, the elliptical model can predict the onset of symmetric vortex merger within 1% of the observed inter-centroid separation (Legras & Dritschel 1991). In three dimensions, a model with similar quantitative accuracy would be especially useful since a direct determination of the conditions for vortex merger and other strong interactions is difficult due to the greater number of parameters (e.g. vertical offset, vortex height-to-width aspect ratio, etc.) and the markedly greater numerical cost of three-dimensional numerical calculations.

Another useful extension would be to permit a variable distribution of PV by nesting ellipsoids as done previously with ellipses in the two-dimensional elliptical model (cf. Legras *et al.* 2001 and references therein). Such nested vortices are not generally exact solutions, but their two-dimensional analogues are in practice excellent approximations to variable-PV vortices. This extension would permit one to study, in a simple approximate way, the erosion or stripping of low-level peripheral PV from vortices by strain and shear, as was done in the two-dimensional context by Legras *et al.* (2001). This would allow one to determine the approximate conditions required for the onset of stripping and the PV profile characteristics which are resistant

to stripping in a arbitrary background flow. Considering the number of parameters involved (three for the background flow alone), a direct attack using the full equations would be prohibitively expensive.

Also, it would be worth investigating the class of inversion operators which may feature in the motion of an ellipsoid. Up to now, only Laplace's operator has been considered. This operator gives rise to a linear, self-induced flow field inside the ellipsoid, through the relations  $\nabla^2\psi_v = q_v$  and  $\mathbf{u}_v = \mathcal{L}\nabla\psi_v$  (where  $\mathcal{L}$  is a  $3 \times 3$  constant matrix). This, and the local linearity of the background flow, are sufficient for the evolution equation (18) for  $\mathcal{B}$  to hold. Clearly, however, the flow need be linear only at the surface of the ellipsoid, so in principle other operators are possible. The operator prescription of the velocity field is itself not necessary – a prescription of the surface flow field as a function of the ellipsoid shape ( $\mathcal{B}$ ) is sufficient.

This paper has focused on situations in which the velocity is induced by the instantaneous shape of the ellipsoid. However, one can imagine other situations, for instance in which the boundary of the ellipsoid is accelerated according to its instantaneous shape. Indeed, much of the early work on this subject concerned the gravitational oscillations of an ellipsoidal body of uniform density, modelling a galaxy, a star or a planet (Todhunter 1873). Here the Laplacian also features in determining the gravitational potential from the mass density, and the gradient of this potential gives the acceleration of the surface. In this application, discussed in Chandrasekhar (1969) and references therein, the evolution equations are second order in time. A similar situation arises for uniformly charged bodies in an electromagnetic field.

The motion of an ellipsoid is seen to be governed by a simple low-order dynamical system. This is elegant, but is it useful? Its importance depends on its robustness. In other words, in the full equations of motion, do non-ellipsoidal disturbances significantly disturb the underlying ellipsoidal dynamics? For the quasi-geostrophic equations, this is an open question, but our simulations of QG turbulence and of individual vortex interactions indicate that vortices often exhibit a near-ellipsoidal shape, most often of a slightly oblate spherical form (Reinaud *et al.* 2003). Moreover, it can be shown that ellipsoids with a circular horizontal cross-section – in the absence of a background flow – are stable to finite-amplitude disturbances (Dritschel 1988). This, together with the well-known (though generally unproven) robustness of two-dimensional elliptical vortices in typical background flows suggests at least comparable robustness for three-dimensional ellipsoidal vortices.

One may also ask what effect departures from the idealized quasi-geostrophic model might have on the robustness of the ellipsoidal approximation. For instance, in the full Boussinesq equations for a stratified rotating fluid, can vortices be well-modelled by ellipsoids? A fundamentally new effect, not present under the quasi-geostrophic approximation, is the radiation of internal gravity waves. This radiation occurs for all vortices having a non-circular horizontal cross-section and probably does not preserve an initially ellipsoidal vortex shape. However, this radiation tends to be weak except under strongly ageostrophic conditions, rarely encountered in the Earth's atmosphere and oceans. Hence, it may be possible to extend the present ellipsoidal approximation to more realistic fluid dynamical models.

#### REFERENCES

- CHANDRASEKHAR, S. 1969 *Ellipsoidal Figures of Equilibrium*. Dover.  
 DRITSCHEL, D. G. 1988 Nonlinear stability bounds for inviscid, two-dimensional, parallel or circular flows with monotonic vorticity, and the analogous three-dimensional quasi-geostrophic flows. *J. Fluid Mech.* **191**, 575–582.

- DRITSCHEL, D. G. 1995 A general theory for two-dimensional vortex interactions. *J. Fluid Mech.* **293**, 269–303.
- DRITSCHEL, D. G. 1999 Scale ratios in decaying quasi-geostrophic turbulence. *Il Nuovo Cimento* **22**, 867–874.
- DRITSCHEL, D. G. 2002 Vortex merger in rotating stratified flows. *J. Fluid Mech.* **455**, 83–101.
- DRITSCHEL, D. G. & DE LA TORRE JUÁREZ, M. 1996 The instability and breakdown of tall columnar vortices in a quasi-geostrophic fluid. *J. Fluid Mech.* **328**, 129–160.
- DRITSCHEL, D. G., DE LA TORRE JUÁREZ, M. & AMBAUM, M. H. P. 1999 On the three-dimensional vortical nature of atmospheric and oceanic flows. *Phys. Fluids* **11**, 1512–1520.
- DRITSCHEL, D. G. & WAUGH, D. W. 1992 Quantification of the inelastic interaction of two asymmetric vortices in two-dimensional vortex dynamics. *Phys. Fluids A* **4**, 1737–1744.
- DRITSCHEL, D. G. & ZABUSKY, N. J. 1996 On the nature of vortex interactions and models in unforced nearly-inviscid two-dimensional turbulence. *Phys. Fluids* **8**, 1252–1256.
- GILL, A. E. 1982 *Atmosphere-Ocean Dynamics*. Academic.
- HASHIMOTO, H., SHIMONISHI, T. & MIYAZAKI, T. 1999 Quasigeostrophic ellipsoidal vortices in a two-dimensional strain field. *J. Phys. Soc. Japan* **68**, 3863–3880.
- KIDA, S. 1981 Motion of an elliptical vortex in a uniform shear flow. *J. Phys. Soc. Japan* **50**, 3517–3520.
- LEGRAS, B. & DRITSCHEL, D. G. 1991 The elliptical model of two-dimensional vortex dynamics. Part I: The basic state. *Phys. Fluids A* **3**, 845–854.
- LEGRAS, B., DRITSCHEL, D. G. & CAILLOL, P. 2001 Erosion of a distributed two-dimensional vortex in a strain flow. *J. Fluid Mech.* **441**, 369–398.
- MEACHAM, S. P., MORRISON, P. J. & FLIERL, G. R. 1997 Hamiltonian moment reduction for describing vortices in shear. *Phys. Fluids* **9**, 2310–2328.
- MEACHAM, S. P., PANKRATOV, K. K., SHCHEPETKIN, A. F. & ZHMUR, V. V. 1994 The interaction of ellipsoidal vortices with background shear flows in a stratified fluid. *Dyn. Atmos. Oceans* **21**, 167–212.
- MIYAZAKI, T., FURUICHI, Y. & TAKAHASHI, N. 2001 Quasigeostrophic ellipsoidal vortex model. *J. Phys. Soc. Japan* **70**, 1942–1953.
- MIYAZAKI, T., UENO, K. & SHIMONISHI, T. 1999 Quasigeostrophic, tilted spheroidal vortices. *J. Phys. Soc. Japan* **68**, 2592–2601.
- MOORE, D. W. & SAFFMAN, P. G. 1971 *Aircraft Wake Turbulence and its Detection*. Plenum.
- REINAUD, J. N. & DRITSCHEL, D. G. 2002 The merger of vertically offset quasi-geostrophic vortices. *J. Fluid Mech.* **469**, 287–315.
- REINAUD, J. N., DRITSCHEL, D. G. & KOUDELLA, C. R. 2003 The shape of vortices in quasi-geostrophic turbulence. *J. Fluid Mech.* **474**, 175–192.
- TODHUNTER, I. 1873 *History of the Mathematical Theories of Attraction and the Figure of the Earth*. London: Constable (reprinted by Dover 1962).